ORGANOMETALLICS

Article

pubs.acs.org/Organometallics

Versatile $Ln_2(\mu\text{-NR})_2$-Imide Platforms for Ligand Exchange and Isoprene Polymerization

Dorothea Schädle, Christoph Schädle, David Schneider, Cäcilia Maichle-Mössmer, and Reiner Anwander*

Department of Chemistry, University of Tübingen, Auf der Morgenstelle 18, 72076 Tübingen, Germany

Supporting Information

ABSTRACT: Bimetallic rare-earth-metal imide complexes $Ln_2(\mu_2\text{-Ndipp})(\mu_3\text{-Ndipp})[(\mu_2\text{-Me})_2AlMe](AlMe_4)_2$ (**3**-Ln; Ln = Y, La, Ce, Nd; dipp = 2,6-diisopropylphenyl) have been obtained from the reaction of $Ln(AlMe_4)_3$ (**1**-Ln) with Li(NHdipp) (**2**). X-ray diffraction studies of toluene-soluble **3**-Ln revealed an unusual $Ln[\{(\mu_2\text{-Me})_2AlMe\}(\mu_3\text{-Ndipp})]Ln$ moiety as the most striking feature. Facile salt-metathetical exchange of the tetramethylaluminato ligands in **3**-Ln with K(L) (L = $N(SiMe_3)_2$, Cp′) allowed for the isolation of $Ln_2(Ndipp)_2[N(SiMe_3)_2]_2(AlMe_3)$ (**4**-La), partially exchanged $Ln_2(Ndipp)_2(Cp')(AlMe_4)(AlMe_3)$ (**5**-La, Cp′ = $C_5Me_4SiMe_3$), and $Ln_2(Ndipp)_2(Cp')_2(AlMe_3)$ (**6**-La). Attempted cleavage of the $AlMe_3$ moiety in **3**-Ln with THF led to C−H bond activation of one of the isopropyl methine moieties to produce $Ln_2(\mu_2\text{-Ndipp})[(\mu_3\text{-}NC_6H_3\text{-}2\text{-}CMe_2\text{-}6\text{-}iPr)Al(\mu_2\text{-Me})_2](AlMe_4)_2$ (**7**-La). Selective cleavage of the bridging $AlMe_3$ "cap" was achieved by addition of DMAP (DMAP = 4-dimethylaminopyridine) to produce $[Ln(\mu_2\text{-Ndipp})(AlMe_4)(DMAP)]_n$ (**8**-Ln; Ln = La, Ce) and concomitantly DMAP·$AlMe_3$. The organoaluminum-free compounds $[Ln(\mu_2\text{-Ndipp})\{N(SiMe_3)_2\}(DMAP)]_2$ (**9**-Ln; Ln = La, Ce), $[Ln(\mu_2\text{-Ndipp})(Cp')(DMAP)]_2$ (**10**-La), and $[Ln(\mu_2\text{-Ndipp})(OAr)(DMAP)]_2$ (**11**-Ln; Ln = La, Ce; Ar = 2,6-di-*tert*-butyl-4-methylphenyl) were obtained via reactions of **8**-Ln with K(L) (L = Cp′, $N(SiMe_3)_2$, OAr). In the presence of activators $[Ph_3C][B(C_6F_5)_4]$ and $[PhNMe_2H][B(C_6F_5)_4]$, $AlEt_2Cl$ complexes **3**-Ln, **5**-Ln, and **7**-Ln initiate the polymerization of isoprene to yield PIPs with narrow molecular weight distributions, involving new imido-supported bimetallic catalysts.

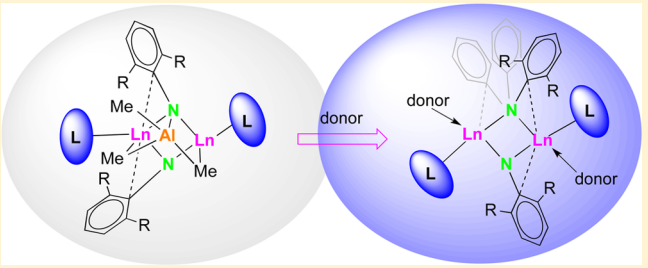

INTRODUCTION

Dianionic cyclooctatetraenyl and pentalene derivatives are categorized as robust ligand platforms (Chart 1), implying unique reactivity and coordination chemistry.[1−4] Similarly, the ubiquitous imido group (NR^{2-}) exhibits an important dianionic ancillary ligand but can also engage in a plethora of cycloaddition reactions (e.g., with alkenes, nitriles, and carbon dioxide as substrates) and (catalytic) metathetical reactions (Wittig-type chemistry).[5−7] Crucially, in high-oxidation-state transition-metal chemistry, the imido functionality has proven particularly useful as a supporting ligand for studying olefin metathesis[8−10] and polymerization reactions.[11,12] In contrast, early-transition-metal imide complexes, in particular group 3[13,14] and group 4 derivatives,[5,15] feature a highly polarized metal−N(imido) bond, which combined with steric unsaturation imparts enhanced reactivity. This has been impressively demonstrated for titanium-promoted transformations such as the catalytic hydroamination of alkynes and imine metathesis.[6]

Chart 1. Routinely Employed Rigid Dianionic Ligands

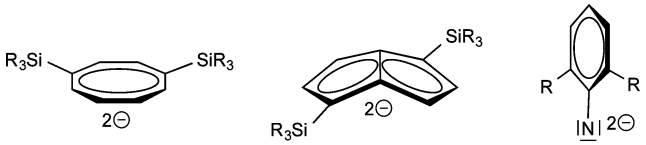

In the realm of the emerging mono-rare-earth-metal (Ln) imide chemistry, both low-coordinate transient[16−18] and isolated terminal Sc^{III}=NR moieties[19] revealed unprecedented reactivity, as exemplified by the functionalization of pyridine with isonitriles to yield mono-imino- and bis-imino-substituted pyridines[18] and the activation of C−H bonds of terminal alkenes and fluoro-substituted alkanes under mild conditions.[20] Reactive rare-earth-metal−main-group-element multiple bonds can be efficiently stabilized in the presence of Lewis acids, as predominantly shown for trimethylaluminum adducts of Ln^{III}−(CH_2^{2-}),[21−29] Ln^{III}−(CH^{3-}),[21,26,30,31] and Ln^{III}−(NR^{2-})[16,32−36] moieties. The first Ln^{III}−Al^{III} bimetallic imide complex was initially observed by Evans et al. when isolating $[(AlMe_4)_2Nd(\mu_3\text{-NPh})(\mu\text{-Me})AlMe]_2$ (**A**, Chart 2) from the reaction of excess $AlMe_3$ with $Nd(NHPh)_3(KCl)_3$.[32] Deliberately, adopting the idea that methylaluminum reagents are capable of deprotonating anilides, Gordon et al. described the dimeric amido-imido samarium compound $[(\mu\text{-ArN})Sm(\mu\text{-NHAr})(\mu\text{-Me})AlMe_2]_2$ (**B**).[33] Similarly, Mindiola et al. obtained the Lewis acid stabilized monoscandium complex $(PNP)Sc(\mu\text{-NAr})(\mu\text{-Me})AlMe_2]$ (**C**, PNP = N[2-P$(CHMe_2)_2$-4-methylphenyl]$_2$, Ar = $C_6H_3iPr_2$-2,6) by treatment of the respective primary amide complex with $AlMe_3$.[16]

Received: July 9, 2015
Published: September 21, 2015

DOI: 10.1021/acs.organomet.5b00589
Organometallics 2015, 34, 4994−5008

Chart 2. Ln(III)−Al(III) Bimetallic Imide Complexes Authenticated by X-ray Structure Analysis

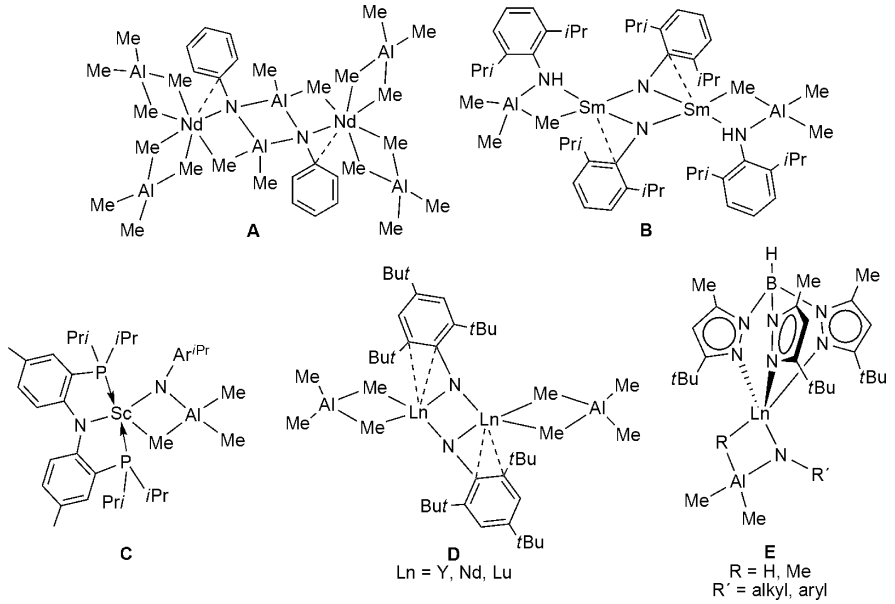

Scheme 1. Synthesis of Imide Complexes 3-Ln−8-Ln

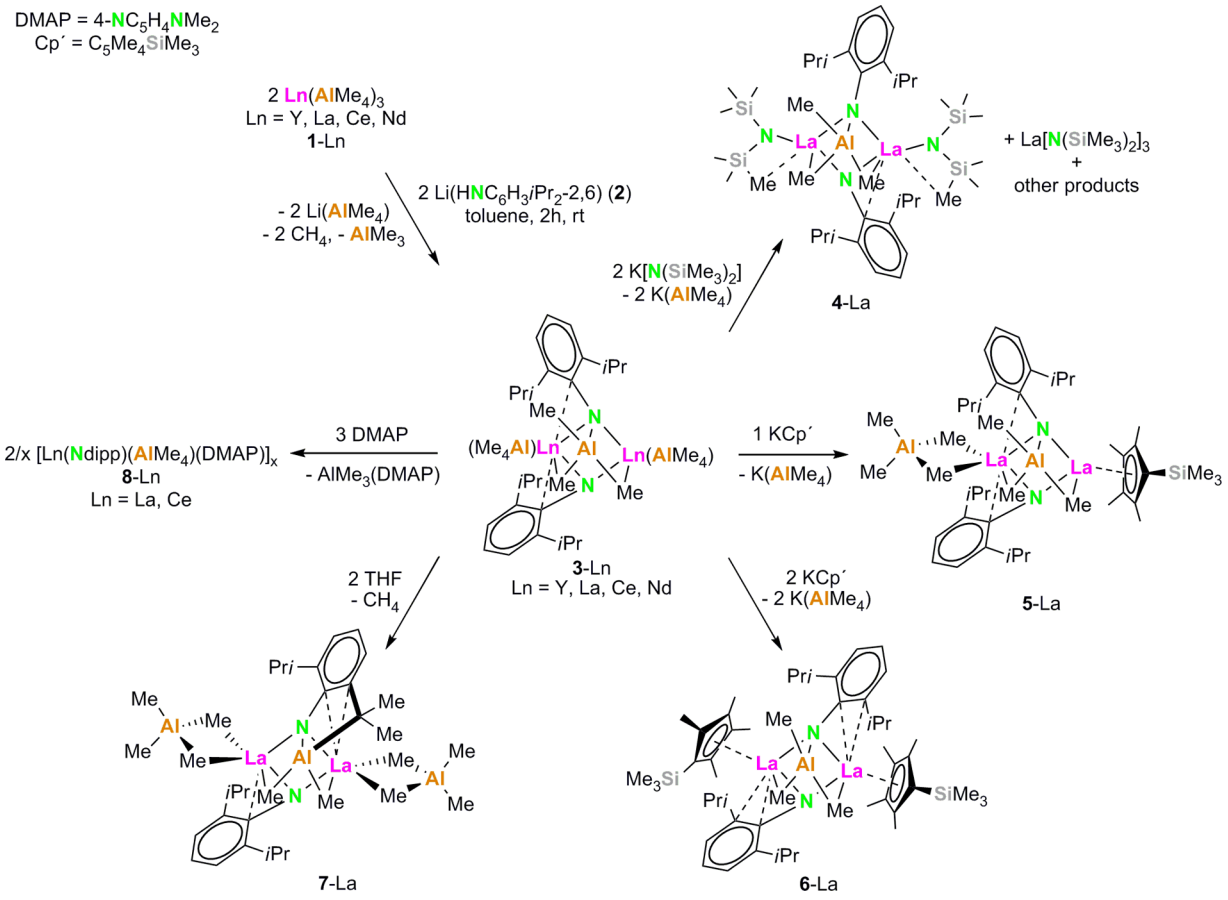

We have recently embarked on an organoaluminum-assisted formation of rare-earth-metal imide complexes using methylaluminate precursors. Accordingly, monomeric (**E**),[34−36] dimeric, and tetrameric (not shown in Chart 2) Lewis acid stabilized rare-earth-metal imides (**D**)[37] could be isolated, depending on the presence of ancillary ligands (use of homoleptic versus heteroleptic alkylaluminates) and the size of the rare-earth-metal(III) center. A key objective of our strategy is to stabilize the imido unit while providing sufficient access to the coordination sphere of the metal to systematically investigate fundamental issues of reactivity. In this work we give a comprehensive account of the synthesis and structural characterization of heteroleptic lanthanum and cerium imide complexes, paying particular attention to (a) variation of the

DOI: 10.1021/acs.organomet.5b00589
Organometallics 2015, 34, 4994−5008

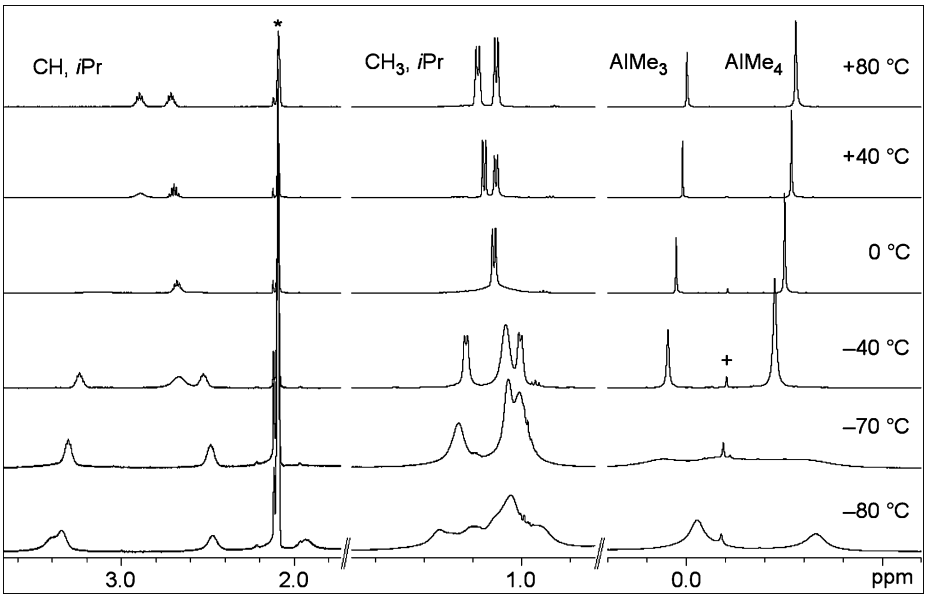

Figure 1. Variable-temperature ^{1}H NMR spectra (500 MHz) of **3**-La, in the region of the metal-bonded alkyl groups and C*H* and CH_3 *i*Pr groups: (*) [D_8]toluene; (+) minor impurity.

ligand sphere by unmasking the imido moiety (full removal of organoaluminum groups), (b) overall ligand exchange, and (c) the catalytic performance of such imido-supported complexes in 1,3-diene polymerization.

RESULTS

Synthesis of Lewis Acid Stabilized Ln(III) Imide Complexes Capable of Ligand Exchange. We focused on complexes of the type **D** as potential precursors due to the presence of reactive $AlMe_4^-$ ligands accessible to protonolysis and salt metathesis reactions alike. Unfortunately, the previously described μ_2-imide complexes $[Ln(AlMe_4)(\mu_2\text{-Nmes*})]_2$ (Ln = Y, Nd, Lu) and $[La(AlMe_4)(\mu_2\text{-Nmes*})]_4$ (mes* = $C_6H_2tBu_3$-2,4,6) were insoluble in aliphatics and dissolved in toluene only at elevated temperatures.[37] Much to our delight, switching to the $Ndipp^{2-}$ ligand (dipp = $C_6H_3iPr_2$-2,6) markedly increased the solubility of the envisaged complexes. The bimetallic rare-earth-metal imide complexes $Ln_2(\mu_2\text{-Ndipp})(\mu_3\text{-Ndipp})[(\mu_2\text{-Me})_2AlMe](AlMe_4)_2$ (**3**-Ln; Ln = Y, La, Ce, Nd) are accessible in high yields by applying a salt metathesis−protonolysis tandem reaction using homoleptic $Ln(AlMe_4)_3$ (**1**-Ln)[38,39] and lithium 2,6-diisopropylphenylamide (**2**) in toluene at ambient temperature (Scheme 1). The ^{1}H NMR and $^{13}C\{^1H\}$ NMR spectra of **3**-La (C_6D_6 at ambient temperature) show two sets of signals for the dipp groups and a higher CH_3/NR ratio as expected for **D**-type complexes, indicating the presence of an additional methylaluminum moiety. Consistent with the molecular drawing of **3**-Ln and the solid-state structure (vide infra), the aluminum-free imido unit and the μ_3-Ndipp moiety bound to a capping $(\mu\text{-Me})_2AlMe$ unit might display distinct chemical shifts. Unfortunately, variable temperature (VT) ^{1}H NMR spectra or NOESY experiments excluded unambiguous assignment (see Figure 1 and Figures S10−S12 in the Supporting Information). However, the ^{1}H NMR spectrum of the C−H activated compound **7**-La (vide infra) provided valuable information, from which we concluded that in **3**-La the broad singlet at 2.90 ppm can be assigned to the isopropyl CH of the μ_3-Ndipp imido ligand and the sharp septet observed at 2.70 ppm to the aluminum-free μ_2-Ndipp unit. Nevertheless, VT ^{1}H NMR studies performed in toluene-d_8 provided some insights into the fluxional behavior of **3**-La in solution, which is affected by at least three dynamic processes: that is, the mobility of the $AlMe_3$ cap, rotation of the aryl groups around the $N_{imido}-C_{ipso}$ bond, and bending of the aryl groups (Figure 1). At 80 °C the isopropyl groups in **3**-La appear as two septets and two sharp doublets. The $AlMe_4$ and $AlMe_3$ moieties of **3**-La display sharp singlets at −0.46 ppm (24H) and 0.06 (9H), respectively, at ambient temperature, while upon cooling to −70 °C the high-field signal decoalesced into two broad singlets. This signal splitting is proposed to originate from distinct chemical evironments of the $AlMe_4$ ligands caused by the positioning of the dipp moieties. Aluminate signal splitting due to restricted methyl group mobility (distinct signals for bridging and terminal methyl groups for both $(\mu\text{-Me})_2Al(Me)_2$ and $(\mu\text{-Me})_3Al(Me)$ moieties) can be ruled out due to the high fluxionality of the methyl groups, as evidenced for homoleptic $La(AlMe_4)_3$ by MAS NMR spectroscopy even in the solid state.[21] At temperatures <−70 °C the [$AlMe_3$] resonance only merged with the low-field [$AlMe_4$] signal, indicating a highly dynamic behavior in solution. This finding is in accordance with the NOESY experiment, where cross-coupling of the trimethylaluminum unit to all isopropyl groups could be detected. At −80 °C the C*H*iPr_2 protons appeared at 3.40, 3.34, 2.47, and 1.93 ppm.

Compounds **3**-Ln are reasonably soluble in *n*-hexane and readily dissolve in toluene. Accordingly, single crystals obtained from saturated *n*-hexane/toluene solutions at ambient temperature revealed isomorphous, triclinic structures for **3**-Ln[a] (Ln = La, Ce, Nd), but when **3**-La was crystallized from an *n*-hexane/toluene mixture at −35 °C, a monoclinic species was obtained (**3**-La[b]). Like complex **D**, the solid-state structures of **3**-Ln (Ln = La, Ce, Nd) feature an asymmetric Ln_2N_2 core, except that one additional neutral $[(\mu\text{-Me})_2AlMe]$ unit is bridging the two rare-earth-metal centers and one imido nitrogen atom (Figure 2, Table 1, and Figures S1 and S2 in the Supporting Information). Overall, the respective La−C(μ-Me) bond lengths (**3**-La: 2.744(4)−3.034(4) Å) are comparable to

DOI: 10.1021/acs.organomet.5b00589
Organometallics 2015, 34, 4994−5008

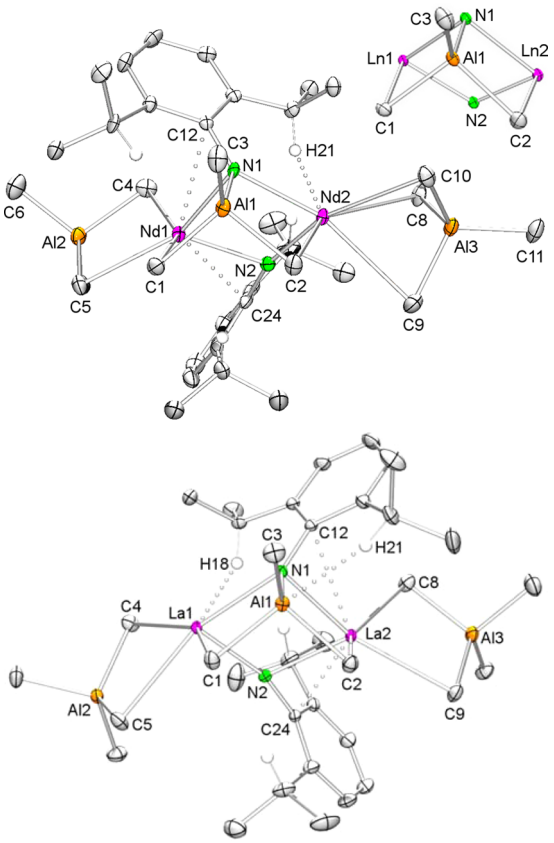

Figure 2. ORTEP representations of the molecular structures of **3**-Nd[a] including the core structure (top), and **3**-La[b] (bottom) with atomic displacement parameters set at the 50% level. Hydrogen atoms, except isopropyl CH, are omitted for clarity. Selected bond lengths and angles are given in Table 1.

Table 1. Selected Distances (Å) and Angles (deg) for $[Ln_2(\mu_2\text{-Ndipp})(\mu_3\text{-Ndipp})[(\mu_2\text{-Me})_2AlMe](AlMe_4)_2]$ (3-Ln; Ln = La, Ce, Nd)

	3-La[a]	3-La[b]	3-Ce[a]	3-Nd[a]
Ln1−N1	2.454(2)	2.516(1)	2.465(3)	2.400(3)
Ln1−N2	2.342(2)	2.212(1)	2.172(3)	2.309(3)
Ln2−N1	2.514(2)	2.473(1)	2.440(3)	2.420(3)
Ln2−N2	2.223(2)	2.358(1)	2.348(3)	2.150(3)
Ln1−C1	2.857(2)	2.742(2)	2.690(4)	2.920(4)
Ln2−C2	2.743(2)	2.855(2)	2.950(4)	2.660(4)
Ln1−C4	2.761(2)	2.831(2)	3.038(3)	2.650(4)
Ln1−C5	2.845(2)	2.873(2)	2.997(4)	2.720(4)
Ln2−C8	3.028(2)	2.718(2)	2.676(4)	2.985(4)
Ln2−C9	2.912(2)	2.836(2)	2.750(4)	2.956(4)
Ln2−C10	3.004(2)		2.946(5)[c]	2.971(4)
av Ln···Al1	3.2731(6)	3.2713(5)	3.251(1)	3.210(1)
Ln1···Al2	3.3665(6)	3.3954(6)	3.075(1)	3.231(1)
Ln2···Al3	3.0758(8)	3.3399(6)	3.279(1)	3.036(1)
Al1−N1	1.898(2)	1.894(1)	1.909(3)	1.904(3)
Ln1−N1−Ln2	95.53(5)	94.99(4)	95.3(1)	94.7(1)
Ln1−N2−Ln2	107.33(6)	107.13(5)	106.5(1)	105.3(1)

[a]Triclinic, space group $P\bar{1}$. [b]Monoclinic, space group $P2_1\bar{c}$. [c]Ce1−C6.

those found in La/Al heterobimetallic complexes featuring carbide, methine, or methylene moieties along with $AlMe_3$ units.[21] The aryl rings of the organoimido ligand are oriented to one side of the molecule, forming secondary interactions with the lanthanide metal centers. As a result, one Ln(III) center of the dilanthanum complex is shielded by the aryl rings through Ln(III)···arene interactions and a η^2-coordinated aluminato ligand with an almost planar $Ln(\mu\text{-Me})_2Al$ moiety, with average $Ln-C(\mu_2\text{-Me})$ bond lengths being slightly longer than those reported for the corresponding homoleptic complexes (**3**-La[a], 2.803 Å; **3**-La[b], 2.777 Å; **3**-Ce[a], 2.713 Å; **3**-Nd[a], 2.685 Å).[39,40] Consequently, the other rare-earth-metal center is protected by the second tetramethylaluminato ligand, which is either η^2-coordinated (average $Ln-C(\mu_2\text{-Me})$: **3**-La[b], 2.852 Å) or η^3-coordinated (average $Ln-C(\mu_2\text{-Me})$: **3**-La[a], 2.981 Å; **3**-Ce[a], 2.993 Å, **3**-Nd[a], 2.971 Å) and features one close contact to one isopropyl methine hydrogen atom (**3**-La[a], La2···H21 = 2.41 Å; **3**-La[b], La1···H18 = 2.43 Å; **3**-Ce[a], Ce1···H21 = 2.37 Å; **3**-Nd[a], Nd1···H21 = 2.34 Å). The η^3 coordination mode is rare but has been observed previously for highly unsaturated Ln(III) centers.[26,31,39,41]

Apparently, the presence of an additional molecule of $AlMe_3$ markedly enhances the solubility of such μ_2-imide complexes $[Ln(AlMe_4)(NR)]_2$. The "trimethylaluminum cap" cannot be simply removed by applying vacuum. In contrast, addition of excess $AlMe_3$ to **3**-La, as probed in C_6D_6 under ambient conditions by ^1H NMR spectroscopy, resulted in a La→Al imido transfer, affording a mixture of $La(AlMe_4)_3$ and $[MeAl\text{-}Ndipp]_3$ (see Figures S13 and S14 in the Supporting Information). This underpines the strong affinity of Al(III) for nitrogen-based ligands,[26,42−46] at the same time opening a new avenue for the synthesis of imidoalanes (see Scheme 2).[47,48] Usually the synthesis of imidoalanes requires prolonged thermal treatment of $AlMe_3$ with H_2NR.[47] The most important application of amidoalanes and imidoalanes is their use as precursors for chemical vapor deposition (CVD) for the production of semiconducting microelectronic devices.[49]

Scheme 2. Reactivity of 3-La toward Trimethylaluminum

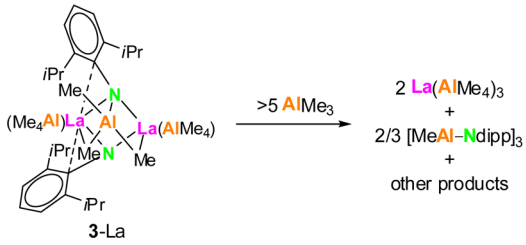

Tetramethylaluminate Ligand Exchange Reactions I. While ligand exchange reactions have been studied for Ln(III) phosphinidene complexes,[50−52] there are no examples for the lighter homologues. Having now a promising precursor at hand, we initially examined the reactivity of **3**-Ln toward archetypal KL (L = $N(SiMe_3)_2$, $C_5Me_4SiMe_3$ = Cp′). Accordingly, the equimolar reaction of **3**-La with $K[N(SiMe_3)_2]$ at −35 °C yielded $Ln_2(Ndipp)_2[N(SiMe_3)_2]_2(AlMe_3)$ (**4**-La), isolable in low yields by fractional crystallization from toluene. The isolation of pure compound **4**-La is hampered by the simultaneous formation of homoleptic amide complex $La[N(SiMe_3)_2]_3$ and other intractable products. The ^1H and $^{13}C\{^1H\}$ NMR spectra of complex **4**-La in C_6D_6 show two sets of signals for the diisopropylphenyl substiutents, accounting for the different chemical environments caused by either the $[(\mu\text{-Me})_2AlMe]$ cap or the aryl ring orientation. Two overlapping singlets at 0.07 ppm in the proton NMR spectrum can be assigned to the $AlMe_3$ unit and the $SiMe_3$ groups of the

DOI: 10.1021/acs.organomet.5b00589
Organometallics 2015, 34, 4994−5008

amido ligand. Decomposition of compound **4**-La is observed within 24 h, as indicated by ^{1}H NMR spectroscopy. Single crystals of **4**-La suitable for X-ray crystallographic analysis were grown from a saturated toluene solution at −35 °C. The unit cell contains four independent molecules, one of which is depicted in Figure 3. All of the molecules feature the same

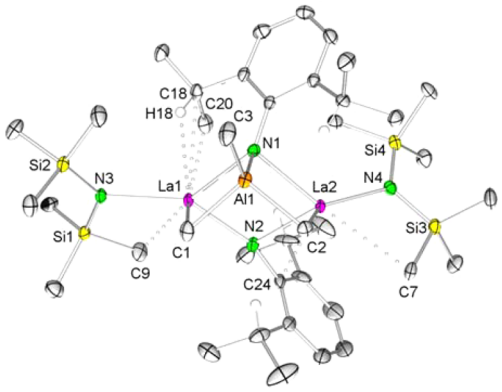

Figure 3. ORTEP representation of the molecular structure of **4**-La with atomic displacement parameters set at the 50% level. Hydrogen atoms (except isopropyl CH) are omitted for clarity. The unit cell contains four independent molecules. The structural data for the other three molecules are shown in the Supporting Information. Selected bond lengths (Å) and angles (deg): La1−N1 2.506(4), La1−N2 2.274(4), La2−N1 2.511(4), La2−N2 2.350(4), La1−N3 2.434(4), La2−N4 2.409(5), La1−C1 2.734 (6), La2−C2 2.908(5), Al1−N1 1.899(5), La1···C18 3.132(6), La1···C20 3.003(6), La2···C24 2.791(5), La1···C9 3.082(5), La2···C7 3.074(5); N2−La2−N4 124.1(2), N1−La1−N3 134.3(1), N2−La1−N3 144.2(1), N1−La1−N4 129.6(2), N1−La1−N2 81.3(2), N1−La2−N2 79.8(1), La1−N1−La2 94.0(1), La1−N2−La2 104.9(2), C1−Al1−C2 99.9(2).

asymmetric orientation of the aryl groups and close secondary interactions of the metal centers with the ipso carbon atoms of the aryl rings, silyl groups, or isopropyl substituents. The La−N(imido) bond lengths vary from 2.252(5) to 2.505(4) Å, suggesting a nonuniform bonding situation in the metallacycle, similar to the case for complex **3**-La and previously reported $[La(Nmes^*)(AlMe_4)]_4$ (mes* = 2,4,6-tri-*tert*-butylphenyl) (La−N(imido) = 2.221(5)−2.414(5) Å).[37]

In order to produce a complex more robust against ligand scrambling reactions, the lanthanum species **3**-La was treated with KCp′. Interestingly, both partially and fully exchanged complexes $Ln_2(Ndipp)_2(Cp')(AlMe_4)(AlMe_3)$ (**5**-La) and $Ln_2(Ndipp)_2(Cp')_2(AlMe_3)$ (**6**-La) were selectively obtained in high yields, depending on whether 1 or 2 equiv of KCp′ was employed. Compounds **5**-La and **6**-La readily dissolve in aromatic solvents but are only slightly soluble in aliphatic hydrocarbons. The ^{1}H NMR spectrum of **5**-La shows two sets of signals in the aromatic region assigned to the protons of the aryl rings, a broad multiplet for the methine groups, two singlets for the Cp′ methyl groups, two broad and one sharp doublet for the isopropyl methyls, and three singlets at 0.41, 0.01, and −0.73 ppm accounting for the $SiMe_3$ group (9H), the $AlMe_3$ unit (9H), and $AlMe_4$ ligands (12H). The $^{13}C\{^{1}H\}$ NMR spectrum displays resonances for the silyl group and the organoaluminum moieties at 2.41 ppm as well as at 2.50 and 1.92 ppm, respectively. The ^{29}Si NMR spectrum of **5**-La obtained by a ^{29}Si DEPT45 experiment showed one sharp signal at δ −11.7 ppm. Complex **6**-La was characterized by ^{1}H, ^{13}C, and ^{29}Si DEPT45 NMR spectroscopy (δ −11.4 ppm), indicating complete exchange of the $AlMe_4$ moieties.

In accordance with NMR spectroscopy, the X-ray crystallographic analysis of **5**-La revealed structural features similar to those found in the solid-state structure of complex **3**-La[a], with one Cp′ ligand substituting the η^3-coordinated $AlMe_4$ ligand (Figure 4). On comparison of **5**-La and **6**-La (Figure 5) with

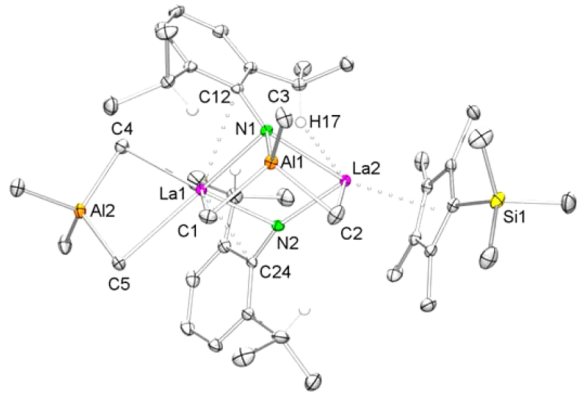

Figure 4. ORTEP representation of the molecular structure of **5**-La with atomic displacement parameters set at the 50% level. Hydrogen atoms (except isopropyl CH) are omitted for clarity. Selected bond lengths (Å) and angles (deg): La1−N1 2.462(1), La1−N2 2.332(1), La2−N1 2.554(1), La2−N2 2.263(1), La1−C1 2.909(2), La2−C2 2.727(2), La1−C4 2.796(2), La1−C5 2.832(2), La2−Ct1 2.584, Al1−N1 1.890(1), Al1−C1 2.048(2), Al1−C2 2.061(2), La1···C12 2.810(2), La1···C24 2.767(2), La2···H17 2.47; N1−La1−N2 78.75(5), N1−La2−N2 78.10(5), La1−N1−La2 95.38(4), La1−N2−La2 107.66(5), La1−N1−C12 88.74(9), La2−N2−C24 160.0(1), C1−Al1−C2 99.81(9), C4−La1−C5−Al2 0.11(6).

homoleptic $LaCp'_3$, the La−Ct (Ct = centroid) distances of 2.593 and 2.608 Å are significantly shorter ($LaCp'_3$ average

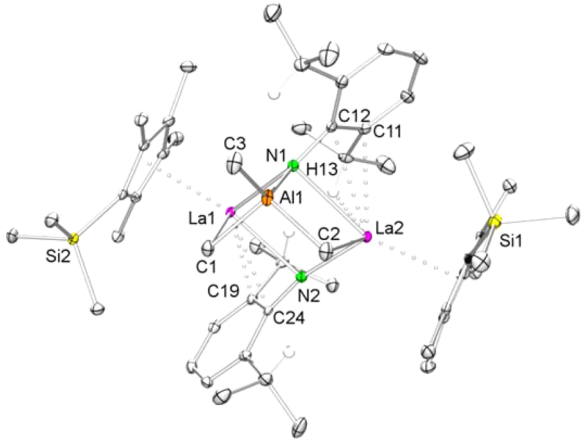

Figure 5. ORTEP representation of the molecular structure of **6**-La with atomic displacement parameters set at the 50% level. Hydrogen atoms (except isopropyl CH) are omitted for clarity. Selected bond lengths (Å) and angles (deg): La1−N1 2.491(2), La1−N2 2.480(3), La2−N1 2.605(3), La2−N2 2.267(2), La1−C1 2.731(3), La2−C2 2.806(3), La1−Ct2 2.608, La2−Ct1 2.593, Al1−N1 1.922(3), Al1−C1 2.026(3), Al1−C2 2.048(4), Al1−C3 1.981(3), La1···C11 2.966(3), La1···C12 2.934(3), La1···C19 3.043(3), La1···C24 2.796(3), La2···H13 2.52; N1−La1−N2 79.77(8), N1−La2−N2 81.42(8), La1−N1−La2 94.36(8), La1−N2−La2 103.81(9), La1−N1−C12 134.9(2), La2−N2−C24 167.8(2), C1−Al1−C2 101.91(15).

DOI: 10.1021/acs.organomet.5b00589
Organometallics 2015, 34, 4994−5008

La−Ct 2.693 Å).[53] Given the distinct ligand arrangements in the solid-state structures of **3**-La[a], **5**-La, and **6**-La, one is tempted to speculate about the mechanism of ligand exchange. In a first step, equimolar $AlMe_4$/Cp′ exchange at the sterically less saturated lanthanum center of the dilanthanum complex (La2 in **3**-La[a]) might occur, producing **5**-La selectively. Substitution of the second $AlMe_4$ ligand by attack of another Cp′ implies realigning of the aryl ring of one imido moiety to the other side. Both aryl rings, which are now directed opposite to each other, feature additional close contacts to the metal centers via the ipso and ortho carbon atoms. The La−N(imido) bond lengths of 2.263(1)−2.554(1) Å (**5**-La) and 2.267(2)−2.605(3) Å (**6**-La) lie well within the expected range; however, they are slightly elongated in comparison to those in the precursor **3**-La.

$AlMe_3$-Decapping Reactions. Aiming at organoaluminum-free heteroleptic imide complexes, we initially treated **3**-La with stoichiometric amounts of tetrahydrofuran (2 equiv). It has been shown previously that ethereal donor molecules can easily cleave off organoaluminum moieties.[54,55] However, the attempted separation of $AlMe_3$ yielded the C−H bond activation product $Ln_2(\mu_2\text{-Ndipp})(\mu_3\text{-NC}_6H_3\text{-2-CMe}_2\text{-6-}i\text{Pr})[Al(\mu_2\text{-Me})_2](AlMe_4)_2$ (**7**-La), involving a $Me_2C{-}Al(\mu_2\text{-Me})_2La$ moiety, as depicted in Scheme 1.[44,56] Compound **7**-La was characterized by ^1H NMR and $^1H^{13}C$ HSQC and HMBC, whereas standard $^{13}C\{^1H\}$ NMR spectroscopy was impeded by subsequent unidentified decomposition reactions in solution. The activation product **7**-La readily dissolved in aromatic solvents but is poorly soluble in *n*-hexane. C−H bond activation of one isopropyl group was corroborated by the ^1H NMR spectrum, where one broad singlet (1H) can be assigned to the intact CH isopropyl group of the $[\mu_3\text{-NC}_6H_3\text{-2-CMe}_2\text{-6-}i\text{Pr}]$ moiety and one sharp septet (2H) to the isopropyl CH protons of the μ_2-Ndipp ligand. Two singlets at −0.13 and −0.39 ppm for the $Al(\mu_2\text{-Me})_2$ moiety indicate magnetically nonequivalent methyl groups.

The dilanthanum structure with the capping $AlMe_2$ unit was unequivocally evidenced by single-crystal X-ray diffraction (Figure 6). Each lanthanum metal center is bonded to a η^2-coordinated, slightly bent $AlMe_4$ ligand (torsion angles La1−C3−Al2−C4 8.1(1)° and La2−C7−Al3−C8 11.3(1)°). As for complexes **3**−**5**, there are distinct imido environments: μ_2 bridging with the imido nitrogen atom being part of a four-membered metallacycle (N2La1N1La2) and μ_3 bridging with the imido nitrogen atom incorporated into two four-membered rings (N1Al1C1La1, N1Al1C2La2) and one five-membered ring (N1Al1C17C13C12) in a propellerlike arrangement. An interesting crystallographic feature of the solid-state structure is the positional disorder of the $Al(\mu_2\text{-Me})_2$ unit connecting the imido CMe_2 group with the lanthanum center. Modeling this positional disorder revealed a statistical ratio of 90:10 (Al1:Al1a) (see the Supporting Information).

Selective cleavage of the $AlMe_3$ unit was achieved via addition of the stronger donor 4-dimethylaminopyridine (DMAP, Steglich's base)[57] to **3**-Ln. Precipitation of "decapped" $Ln(\mu_2\text{-Ndipp})(AlMe_4)(DMAP)]_x$ (**8**-Ln; Ln = La, Ce) facilitated its separation from the toluene-soluble literature-known coproduct DMAP·$AlMe_3$.[58] Complexes **8**-Ln, which are readily soluble in THF as **8**-La·THF but insoluble in aliphatic and aromatic hydrocarbons, can be obtained in moderate yields. The low stability of **8**-La in ethereal solvents, however, is indicated by the presence of three ^1H NMR resonances at −0.76, −0.93, and −1.16 ppm for metal-bonded methyl groups.

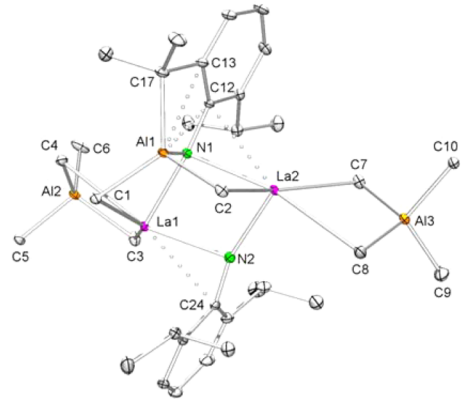

Figure 6. ORTEP representation of the molecular structure of **7**-La with atomic displacement parameters set at the 30% level. Hydrogen atoms and the disorder in the $AlMe_2$ moiety are omitted for clarity. Selected bond lengths (Å) and angles (deg): La1−N1 2.328(2), La1−N2 2.394(2), La2−N1 2.454(2), La2−N2 2.234(2), La1−C1 3.018(3), La2−C2 2.903(3), La1−C3 2.785(2), La1−C4 2.937(2), La2−C7 2.794(3), La2−C8 2.888(2), Al1−N1 1.942(2), Al1−C1 2.004(3), Al1−C2 2.038(3), Al1−C17 1.984(2), Al1···C12 2.698(3), Al1···C13 2.699(2), La1···C24 2.781(2), La2···C12 2.851(2); N1−La1−N2 77.13(7), N1−La2−N2 77.64(7), La1−N1−La2 100.24(7), La1−N2−La2 104.88(8), La1−N2−C24 90.4(1), La2−N1−C12 90.6(1), C1−Al1−C2 106.7(1), La1−C3−Al2−C4 8.1(1), La2−C7−Al3−C8 11.3(1).

Variable-temperature (VT) ^1H NMR studies gave some insights into a possible decomposition pathway. Over the course of a thermal treatment of **8**-La in THF-D_8 (room temperature to +80 °C) the intensities of the resonances assignable to adduct $Me_3Al{\cdot}THF$[59] and La−CH_3 moieties increased at the expense of the educt signals (Figure S31 in the Supporting Information). As for complex **7**-La, $^{13}C\{^1H\}$ NMR spectroscopic studies of **8**-La were hampered by its decomposition in solution. The ^1H NMR spectrum of **8**-Ce in C_6D_6/THF-D_8 was not conclusive, due to the paramagnetic nature of cerium(III). Crystallization from toluene/THF afforded yellow crystals of **8**-La·THF suitable for X-ray diffraction analysis (Figure 7). Each six-coordinate lanthanum center is surrounded by two imido ligands, two THF, one DMAP, and one η^1-coordinated $AlMe_4$ ligand and features one additional close contact to the ipso carbon atom of the aryl ring. The La−N(imido) bond lengths are in accordance with the corresponding metrical parameters observed for the related complex **3**-La but are significantly shorter than the La−N(DMAP) bonds. With regard to the unusual η^1 coordination mode of the $AlMe_4$ ligand, the only comparable structure is the bis(amido)pyridine lanthanum complex $La(AlMe_4)(THF)[NC_5H_5\{CMe_2N\text{-}(C_6H_3i\text{Pr}_2\text{-}2,6)\}_2\text{-}2,6]$,[60] featuring the well-known cleaving agent THF in the same molecule. The terminal η^1 coordination mode is rare but has been observed previously for oversaturated Ln(III) centers.[22,24,35] The average La−C(μ-Me) distance in **8**-La·THF (3.007 Å) is somewhat longer than that in the aforementioned bis(amido)pyridine complex (2.825(7) Å).[60]

Tetramethylaluminate Ligand Exchange Reactions II. As evidenced for complexes **3**-Ln, the $AlMe_4$ ligand in **8**-Ln can be easily replaced by other ligands to yield aluminum-free complexes. Salt-metathesis reactions of **8**-Ln and potassium salts K(L) (L = Cp′, $N(SiMe_3)_2$, $OC_6H_2t\text{Bu}_2$-2,6-Me-4) in toluene at ambient temperature yielded straightforwardly $[Ln(\mu_2\text{-Ndipp})\{N(SiMe_3)_2\}(DMAP)]_2$ (**9**-Ln; Ln = La, Ce),

DOI: 10.1021/acs.organomet.5b00589
Organometallics 2015, 34, 4994−5008

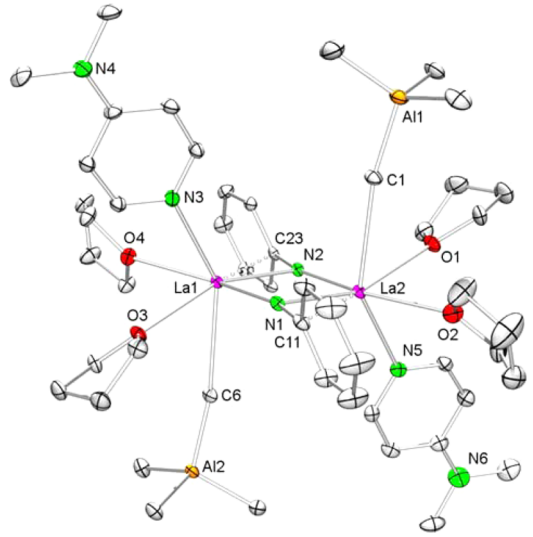

Figure 7. ORTEP representation of the molecular structure of **8**-La·THF with atomic displacement parameters set at the 50% level. Hydrogen atoms and isopropyl groups are omitted for clarity. Selected bond lengths (Å) and angles (deg): La1−N1 2.232(4), La1−N2 2.438(4), La2−N1 2.434(4), La2−N2 2.235(4), La1−N3 2.699(4), La2−N5 2.726(4), La1−C6 3.035(5), La2−C1 2.978(5), La1−O3 2.629(3), La1−O4 2.722(3), La2−O1 2.640(3), La2−O2 2.680(3), La1···C23 2.951(4), La2···C11 2.998(5); N1−La1−N2 81.3(1), N1−La2−N2 81.1(1), La1−N1−La2 98.8(1), La1−N2−La2 98.8(1), La1−N2−C23 97.3(3), La2−N1−C11 99.5(3), C6−La1−N3 148.7(1), C1−La2−N5 146.7(1).

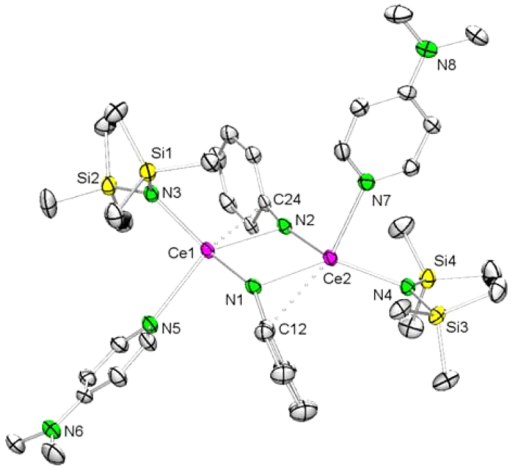

Figure 8. ORTEP representation of the molecular structure of **9**-Ce with atomic displacement parameters set at the 30% level. Hydrogen atoms, isopropyl groups, residual *n*-hexane, disorder in one of the NMe_2 groups, and one silyl group are omitted for clarity. The unit cell contains two independent molecules with similar structural data. The structural data for the other molecules are depicted in the Supporting Information. Selected bond lengths (Å) and angles (deg): Ce1−N1 2.217(3), Ce1−N2 2.411(3), Ce2−N1 2.398(3), Ce2−N2 2.200(3), Ce1−N3 2.409(3), Ce2−N4 2.439(3), Ce1−N5 2.674(3), Ce2−N7 2.615(3), Ce1···C24 2.762(3), Ce2···C12 2.956(3); N1−Ce1−N2 77.91(9), N1−Ce2−N2 78.49(9), Ce1−N1−Ce2 101.7(1), Ce1−N2−Ce2 101.73(10), Ce1−N2−C24 89.43(18), Ce2−N1−C12 99.1(2), N1−Ce1−N5 87.01(9), N2−Ce2−N7 101.75(9), N3−Ce1−N5 95.66(9), N4−Ce2−N7 93.03(9).

$[Ln(\mu_2\text{-Ndipp})(Cp')(DMAP)]_2$ (**10**-La) and $[Ln(\mu_2\text{-Ndipp})(OAr)(DMAP)]_2$ (**11**-Ln; Ln = La, Ce) in high yields. Separation of the byproduct $KAlMe_4$ by filtration afforded the toluene-soluble complexes **9**-Ln−**11**-Ln.

Single crystals of **9**-Ln suitable for X-ray diffraction analysis were grown from toluene solutions at −35 °C, revealing the all-nitrogen coordination sphere of the Ln(III) centers in **9**-Ln (Scheme 3). The molecular structure of compound **9**-Ce is presented in Figure 8. Each Ln(III) center is four-coordinate, adopting a distorted-tetrahedral geometry with two dianionic imido ligands, one monoanionic amido ligand, and one neutral N-donor molecule, which is reflected by a gradual increase in the Ln−N bond lengths. The asymmetry of the Ln_2N_2 core is further manifested by the presence of a significant interaction between the ipso carbon of the bridging μ-Ndipp ligand and one of the lanthanide metal centers Ln···C12/C24. The average Ln−N(imido) bond lengths of 2.334 Å (**9**-La) and 2.308 Å (**9**-Ce), respectively, lie well within the expected range. In fact, the average Ln−N(amido) bond lengths of 2.478 Å (**9**-La) and 2.425 Å (**9**-Ce) compare well with the longer Ln−N(imido) bond lengths. The Ln−N(donor) distances of **9**-Ln (average La−N 2.703 Å, average Ce−N 2.637 Å) match the corresponding values reported for six-coordinate, tetravalent

Scheme 3. Synthesis of Imide Complexes 9-Ln−11-Ln

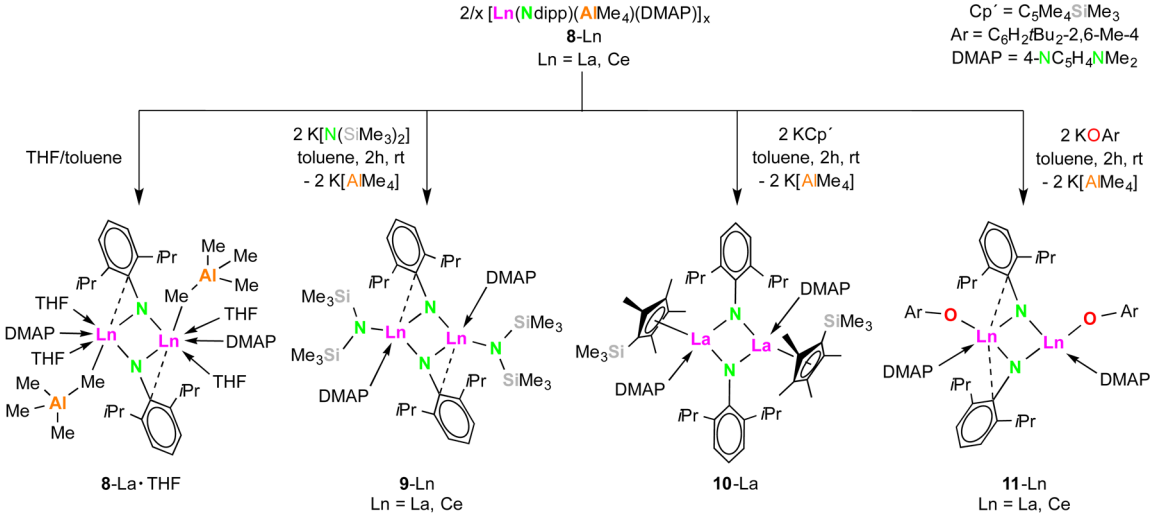

DOI: 10.1021/acs.organomet.5b00589
Organometallics 2015, 34, 4994−5008

complex $Ce(OCMe_2iPr)_4(DMAP)_2$ (average Ce−N 2.668 Å).[61]

Following a similar salt metathetical procedure, **8**-La can be converted into the heteroleptic half-sandwich complex $[Ln(\mu_2\text{-}Ndipp)(Cp')(DMAP)]_2$ (**10**-La) employing KCp′. In the solid state the lanthanum metal centers are formally six-coordinate with bridging imido ligands, and each center has η^5-Cp′ and DMAP ligands (Figure 9). In stark contrast to the structural

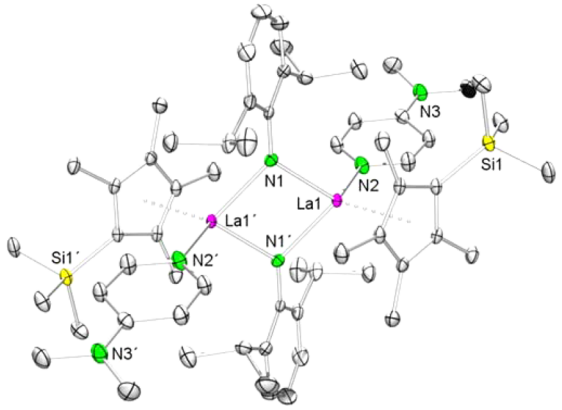

Figure 9. ORTEP representation of the molecular structure of **10**-La with atomic displacement parameters set at the 50% level. Hydrogen atoms are omitted for clarity. Selected bond lengths (Å) and angles (deg): La1−N1 2.347(1), La1−N1′ 2.348(1), La1−N2 2.713(2), La1−Ct1 2.639; La1−N1−C12 129.2(1), N1−La1−N1′ 79.43(5), La1−N1−La1′ 100.57(5).

chemistry of **3**-Ln−**9**-Ln and $[Ln(Nmes^*)(AlMe_4)]_x$[37] (x = 2, Ln = Y, Nd, Lu; x = 4, Ln = La) the X-ray structure analysis of complex **10**-La revealed equally long Ln−N bonds and the absence of La···arene interactions. This symmetry switch of the La_2N_2 metallacycle can be ascribed to the increased steric shielding of the Cp′ ligand. The bonding situation is reflected by medium values for the La−N bond lengths (2.347(1) and 2.348(1) Å, average La−Ct 2.693 Å).[53] As a consequence, the atoms $C12_{ipso}/N1_{imido}/N1'_{imido}/C12'_{ipso}$ are linearly arranged with the aryl rings twisted by an angle of 52.14(5)° against the plane spanned by the metallacycle. The ^1H NMR and $^{13}C\{^1H\}$ NMR spectra of **10**-La in C_6D_6 show only one set of signals for the ligand periphery. The chemical shift of δ 11.9 ppm in the ^{29}Si DEPT45 NMR is in the expected range.

Colorless single crystals of the aryloxide complex **11**-La were grown from a hot benzene solution by slowly cooling it to ambient temperature. X-ray structure analysis revealed four-coordinate La(III) centers and a fan-shaped arrangement of the bridging aryl imido moieties with typical intramolecular La−N_{imido} distances ranging from 2.262(3) to 2.416(3) Å (Figure 10). A striking feature of the solid-state structure of **11**-La is the cis positioning of the DMAP and aryloxo ligands relative to the plane spanned by the metallacycle. The La−$O_{aryloxo}$ bond distances (average La−O 2.271 Å) are similar to those observed for the five-coordinate aryloxide complex $[La(OAr)_3(NCMe)_2]\cdot 2NCMe$ (Ar = 2,6-di-*tert*-butyl-4-methylphenyl, average 2.252(1) Å).[62]

Formation of Active Species for the Polymerization of Isoprene. Well-defined mono-rare-earth-metal-based initiating systems are routinely obtained from complexes $(L1)LnR_2$ (R = alkyl, benzyl, allyl, alkylaluminate), which are stabilized by monoanionic ancillary ligands, upon cationization with the borate activators $[Ph_3C][B(C_6F_5)_4]$ (**A**), $[PhNMe_2H][B(C_6F_5)_4]$ (**B**) (L1, Chart 3), and $B(C_6F_5)_3$ (**C**). The proposed active species **AS1** features a highly electron-deficient Ln(III)

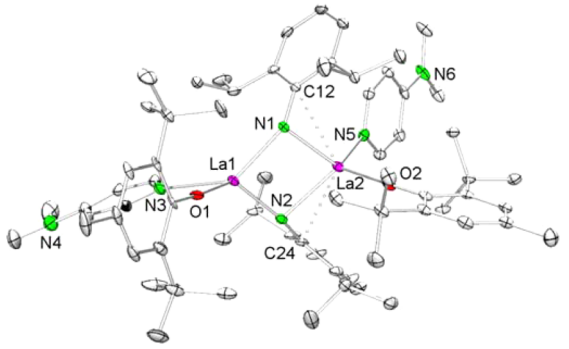

Figure 10. ORTEP representation of the molecular structure of **11**-La with atomic displacement parameters set at the 50% level. Hydrogen atoms are omitted for clarity. Selected bond lengths (Å) and angles (deg): La1−N1 2.275(3), La1−N2 2.262(3), La2−N1 2.363(3), La2−N2 2.416(3), La1−N3 2.75(2), La2−N5 2.641(3), La1−O1 2.398(13), La1−O1A 2.18(2), La2−O2 2.234(3), La2···C12 2.883(4), La2···C24 2.767(4); N1−La1−N2 83.2(1), N1−La2−N2 78.1(1), La1−N1−La2 99.7(1), La1−N2−La2 98.5(1), La2−N1−C12 97.2(2), La2−N2−C24 89.2(2), O1−La1−N3 94.1(7), O2−La2−N5 117.6(1).

Chart 3. Proposed Active Species of Ln(III)-Based 1,3-Diene Polymerization Initiators[a]

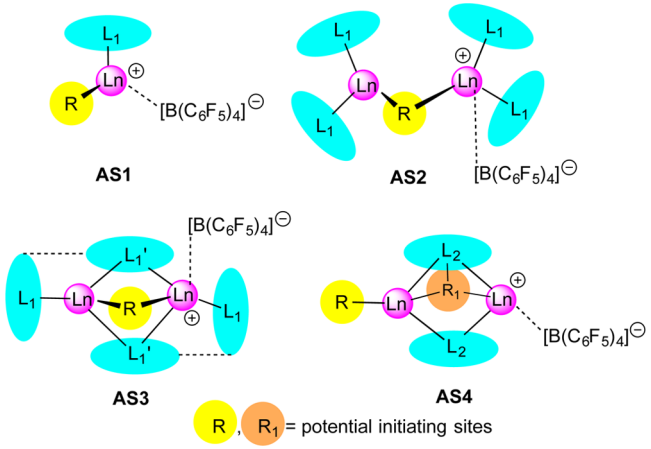

[a]L1(L1′) = (linked) monoanionic ancillary ligands, e.g., cyclopentadienyl; L2 = dianionic ancillary ligand; R = monovalent actor ligand, mainly alkyl.

center bonded to one remaining reactive ligand, which constitutes the initiating site R.[63−69] Well-defined dimeric rare-earth-metal initiators have been far less investigated,[70] although the few reported examples did reveal excellent performance in stereospecific 1,3-diene polymerization. The ternary system $[(C_5Me_4)_2Ln(\mu\text{-}Me)_2AlMe_2]_2$/**A**/Al*i*$Bu_3$, representing the dimeric monoalkyl monocation **AS2**, produced >99% 1,4-*cis*-polybutadiene at −20 °C.[71−73] On the other hand, the constrained-geometry complex $[(C_5Me_4)SiMe_2P(Cy)Ln(CH_2SiMe_3)]_2$ afforded >99% isotactic 3,4-polysioprene polymerization upon activation with **A** (representing **AS3**).[74] Intrigued by such exceptional catalytic performances of dimeric rare-earth-metal alkyl complexes, we examined cationization and chlorination reactions of our dimeric imide complexes $Ln_2(\mu_2\text{-}Ndipp)(\mu_3\text{-}Ndipp)[(\mu_2\text{-}Me)_2AlMe](AlMe_4)_2$ (**3**-Ln; Ln

DOI: 10.1021/acs.organomet.5b00589
Organometallics 2015, 34, 4994−5008

Scheme 4. Proposed Reaction of $Ln_2(\mu_2\text{-Ndipp})(\mu_3\text{-Ndipp})[(\mu_2\text{-Me})_2AlMe](AlMe_4)_2$ (3-La, 3-Ce, 3-Nd) with $[Ph_3C][B(C_6F_5)_4]$ (A) and $[PhNMe_2H][B(C_6F_5)_4]$ (B)

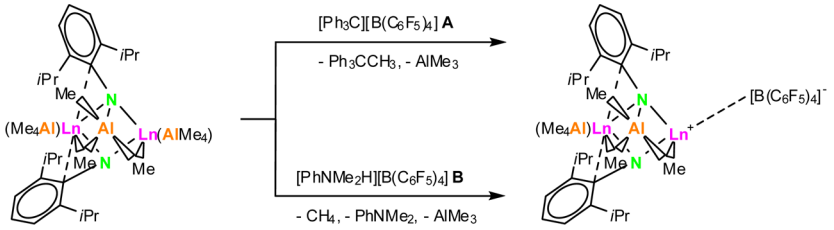

Table 2. Effect of Ln(III) Size and Cocatalyst on the Polymerization of Isoprene

					microstructure[d]				
entry[a]	precat.	cocat.[b]	t (h)	yield (%)[c]	*cis*-1,4	*trans*-1,4	3,4	$10^5 M_n$	M_w/M_n
1	**3**-La	**A**	4	87	30	64	6	0.7	1.28
2	**3**-La	**A**	24	>99	20	74	6	1.8	1.31
3[e]	**3**-La	**A**	4	79	39	54	7	3.4	1.46
4[e]	**3**-La	**A**	24	>99	45	38	17	2.9	1.45
5[f]	**3**-La	**A**	4	95	36	57	7	2.6	1.43
6[f]	**3**-La	**A**	24	>99	36	59	5	2.7	1.40
7	**3**-La	**B**	24	40	33	59	8	0.4	1.97
8	**3**-La	Et_2AlCl	24	63	79	18	3	0.4	1.22
9[e]	**3**-La	Et_2AlCl	24	88	82	13	5	0.6	1.33
10[g]	**3**-La	Et_2AlCl	24	89	80	15	5	0.9	1.35
11	**3**-Ce	**A**	24	>99	27	66	7	1.5	1.43
12	**3**-Ce	**B**	24	46	52	37	11	0.3	2.25
13	**3**-Ce	Et_2AlCl	24	75	90	6	4	0.8	1.38
14	**3**-Nd	**A**	16	> 99	29	63	8	1.1	2.07
15	**3**-Nd	**A**	24	> 99	30	62	8	1.4	1.73
16	**3**-Nd	**B**	24	77	35	50	15	0.8	1.78
17	**3**-Nd	Et_2AlCl	24	77	83	14	3	0.5	1.74
18[e]	**3**-Nd	Et_2AlCl	24	86	80	16	4	0.7	1.41
19[g]	**3**-Nd	Et_2AlCl	24	87	79	16	5	0.3	1.54
20	**5**-La	**A**	24	> 99	16	52	32	0.8	1.39
21[e]	**5**-La	Et_2AlCl	24	80	85	6	9	1.4	1.39
22	**7**-La	**A**	24	41	50	32	18	0.3	2.0
23[e]	**7**-La	**A**	4	30	77	11	12	1.4	1.7
24[e]	**7**-La	**A**	24	99	64	26	10	3.0	1.4

[a]Conditions unless specified otherwise: 0.02 mmol of precatalyst, [Ln]/[cocat] = 1/1, 8 mL of toluene, 20 mmol of isoprene. [b]Cocatalyst: (**A**) $[Ph_3C][B(C_6F_5)_4]$; (**B**) $[PhNMe_2H][B(C_6F_5)_4]$. Catalyst preformation 5 min at ambient temperature. [c]Determined by ^1H and ^{13}C NMR spectroscopy in $CDCl_3$. [d]Determined by means of size-exclusion chromatography (SEC) against polystyrene standards: M_n = number-average molecular weight; M_w = weight-average molecular weight. [e][Ln]/[cocat] = 1/2. [f]Isoprene was added to the catalyst mixture. [g][Ln]/[cocat] = 1/3.

= La, Ce, Nd) as well as their catalytic performance in the polymerization of isoprene dependent on the nature of the cocatalyst. In general, nuclearity and cooperativity effects in binuclear catalysts have attracted considerable attention in olefin polymerization catalysis.[75,76] ^1H NMR monitoring of the reaction of **3**-La with an equimolar amount of $[Ph_3C][B(C_6F_5)_4]$ (**A**) or $[PhNMe_2H][B(C_6F_5)_4]$ (**B**) in C_6D_6 showed the instant disappearance of the signals for the neutral complex **3**-La and the appearance of new signals assignable to Ph_3CCH_3 or $PhNMe_2$ and CH_4, respectively (Scheme 4). Fast reactions are also visually recognized from the immediate decoloration of a yellow solution of **3**-La upon addition of an orange solution of **A**. Instant gas evolution and the formation of a faint colorless solution was observed for the activation with **B**. New signals for the remaining $AlMe_4$ ligand and the bridging $(\mu\text{-Me})_2AlMe$ unit appeared to be shifted to higher field, in accordance with a stronger coordination toward the highly electron deficient lanthanum cation. The $^{11}B\{^1H\}$ NMR spectra of **3**-La/**A** and **3**-La/**B** in C_6D_6 revealed broad resonances at δ −16.0 and −16.5 ppm, respectively. $^{19}F\{^1H\}$ chemical shifts at δ −131.9/−161.6/−165.8 ppm for **3**-La/**A** and **3**-La/**B** can be assigned to the *o*-, *p*-, and *m*-F atoms of the borate. A ^1H NMR spectroscopic study of the reaction of **3**-La and $[PhNMe_2H][B(C_6F_5)_4]$ showed sharp singlets at 0.01, −0.47, and −0.54 ppm, which clearly correspond to one intact $(\mu\text{-Me})_2AlMe$ cap, one $AlMe_4$ ligand, and released $AlMe_3$, respectively (Figure S43 in the Supporting Information). The high-field shift of the last species indicated coordination to *N*,*N*-dimethylaniline. In addition, the chemical shifts of formed $PhNMe_2$ are not consistent with the reported ^1H NMR shifts for free $PhNMe_2$ in C_6D_6. Particularly, the methyl groups resonate at higher field (2.26 ppm) in comparison with free $PhNMe_2$ (2.50 ppm).[77] The comparative ^1H NMR study of **3**-La/**A** revealed one sharp singlet at 0.02 ppm for the $(\mu\text{-Me})_2AlMe$ unit and three broad singlets at −0.14, −0.19, and −0.41 ppm for additional methylaluminum groups as well as four sets of signals for the isopropyl groups, suggesting the formation of a highly asymmetric cationic species or the presence of more than

DOI: 10.1021/acs.organomet.5b00589
Organometallics 2015, 34, 4994−5008

one cationic species. Addition of 1 or 2 equiv of Et_2AlCl to **3**-La in C_6D_6 resulted in the precipitation of white solids, which turned into clear yellow solutions. The ^1H NMR spectrum of the mixture **3**-La/Et_2AlCl indicated the disappearance of the educt signals at the expense of a nonconclusive multisignal NMR spectrum.

In preceding studies on the catalytic performance of N-donor-functionalized cyclopentadienyl,[56] formamidinate,[68,78] and triazenide[46] bis(tetramethylaluminate) complexes we and others demonstrated the high potential of rare-earth-metal complexes bearing N-heteroatom ancillary ligands as initiators for the stereospecific living polymerization of isoprene.[79,80] At the time, we pointed out the propensity of the N-heteroatom ancillary ligands to transfer to organoaluminum compounds,[46] which are routinely used as additional cocatalysts.[81] In this study, however, we report for the first time on the catalytic activity of the new type of di-rare-earth-metal catalyst **AS4**: namely, cationic imide complexes derived from precatalysts $Ln_2(\mu_2\text{-Ndipp})(\mu_3\text{-Ndipp})[(\mu_2\text{-Me})_2AlMe](AlMe_4)_2$. The outcome of the reactions, e.g., yield and stereoregularity, was mainly dependent on the size of the Ln metal center (La(III) versus Ce(III) versus Nd(III)) and the intrinsic properties of the cocatalysts (Table 2; see also the Supporting Information). Complexes **3**-Ln showed moderate to good activity in the polymerization of isoprene upon activation with cocatalyst **A**, and the observed catalyst activities are comparable to those reported for mixtures of triazenide complexes[46] and **A**. The main component of the resulting polyisoprenes (PIP) has trans-1,4 stereoregularity which does not exceed a maximum of 74% for **3**-La/**A** (Table 2, run 2), however, corroborating the trans-directing effect of cocatalyst **A**. Changing the catalyst/cocatalyst ratio from 1/1 to 1/2 increased the cis contents (runs 3 and 4), in agreement with enhanced steric unsaturation at the rare-earth-metal centers. Polymers gained from catalyst mixtures **3**-Ln/**A** show narrow molecular weight distributions (minimum 1.28). The polymerization performance of the binary system **3**-Ln/**B** gave PIP in low to moderate yield with low stereoselectivity. The catalyst system **3**-Ln/**C** either did not polymerize isoprene or did so poorly, which is in accordance with the low activation capability of $B(C_6F_5)_3$ (**C**) found in other catalyst mixtures (Supporting Information).[46] Use of the asymmetrically coordinated complex **5**-La featuring one Cp′ ligand had a major impact on the polymerization performance. The high content of 3,4-PI (32%; Table 2, run 20) is clearly due to the presence of sterically congested metal centers.

In order to compare borate-based cationization with chlorination-based activation protocols, we examined the binary system **3**-Ln/**Et_2AlCl** by applying different ratios of precatalyst and cocatalyst. Upon addition of 1−3 equiv of Et_2AlCl to **3**-La precipitation of a white solid and subsequently the formation of a yellow solution was observed. However, the possible resulting chlorinated species could not be assigned due to the complexity of the ^1H NMR spectrum. Nevertheless, use of a precatalyst/cocatalyst ratio of 1/1 gave a reasonably active initiator system and the crucial cis-directing role of the chloride coligand could be confirmed (90% *cis*-1,4, Table 2, run 13). Addition of 2 equiv of Et_2AlCl to **3**-Ln (2/1) increased the yield of PIP, but addition of a third molecule of Et_2AlCl did not further affect the polymerization performance. The polymerization performance of the chlorinated species (maximum 90% 1,4-cis and molecular weight distributions as narrow as 1.22) suggests that ligand redistribution and formation of homoleptic $Ln(AlMe_4)_3$ does not occur under these conditions. For comparison, the PIPs fabricated by the binary systems $Nd(AlMe_4)_3$ exhibit >98% 1,4-cis and relatively broad molecular weight distributions (2.5−4.5).[82] Finally, the availability of two potential initiating sites in **3**-La-based catalyst mixtures is indicated by the formation of active species when **3**-La/cocatalyst mixtures of ratios of ≥2 were employed. This is in accordance with previous studies on discrete aryl(alk)oxide trimethylaluminum adducts $Ln(OR)_3(AlMe_3)_x$, which revealed the formation of active species for x = 2, 3 but not x = 1 upon activation with Et_2AlCl.[83]

CONCLUSIONS

Bimetallic rare-earth-metal imide complexes $Ln_2(\mu_2\text{-Ndipp})_2[(\mu_2\text{-Me})_2AlMe](L)_2$ and $[Ln(\mu_2\text{-Ndipp})(DMAP)(L)]_2$ (L = $AlMe_4$, $N(SiMe_3)_2$, Cp′, OAr) were synthesized as unique examples to demonstrate that imido ligands can act as ancillary ligands in organolanthanide chemistry. The central $Ln_2(\mu_2\text{-Ndipp})_2$ metallacycle seems resistant to salt-metathetical exchange reactions but does adapt to different steric requirements by distinct aryl bending involving secondary Ln··· arene interactions. The stability of the $Ln_2(\mu_2\text{-Ndipp})_2$ core can also be exploited for catalytic transformations, as shown for 1,3-diene (isoprene) polymerization. Activation of the complexes $Ln_2(\mu_2\text{-Ndipp})_2[(\mu_2\text{-Me})_2AlMe](AlMe_4)_2$ with $[Ph_3C][B(C_6F_5)_4]$ or Et_2AlCl produces moderately active catalysts showing 1,4-*trans*- and 1,4-*cis*-directing behavior, respectively. NMR spectroscopic studies and the polymerization performance, which are different from those of the homoleptic derivatives $Ln(AlMe_4)_3$, suggest the integrity of the $Ln_2(\mu_2\text{-Ndipp})_2$ core during catalyst activation and subsequent polymerization and hence the presence of a new dinulear initiating species (**AS4**).

EXPERIMENTAL SECTION

General Considerations. All operations were performed with rigorous exclusion of air and water, using standard Schlenk, high-vacuum, and glovebox techniques (MBraun 200B; <1 ppm of O_2, <1 ppm of H_2O). Toluene and *n*-hexane were purified by using Grubbs columns (MBraun SPS, solvent purification system) and stored inside a glovebox. C_6D_6 (99.5%) was received from Deutero GmbH and $C_6D_5CD_3$ (99.5%) and C_4D_8O (99.5%) were obtained from Eurisotop. The NMR solvents were dried over Na for a minimum of 48 h and filtered through a filter pipet (Whatman) before use. The primary amine 2,6-diisopropylaniline was obtained from Aldrich, degassed by three freeze−pump−thaw cycles, and stored inside a glovebox over molecular sieves (4 Å); *n*-butyllithium and DMAP were purchased from ABCR and used as received. $K[N(SiMe_3)_2]$ was obtained from Aldrich and used as received. Homoleptic $Ln(AlMe_4)_3$ (**1**-Ln; Ln = Y, La, Ce, Nd) were synthesized according to literature procedures.[38,39] K(OAr) (Ar = 2,6-di-*tert*-butyl-4-methylphenyl)[84] and KCp′ (Cp′ = $C_5Me_4SiMe_3$)[85] were synthesized according to slightly modified literature procedures. H_2Ndipp (dipp = $C_6H_3iPr_2$-2,6) was lithiated with *n*-butyllithium (for a detailed procedure see the Supporting Information). NMR spectra of air- and moisture-sensitive compounds were recorded by using J. Young valve NMR tubes at variable temperature on Bruker AVII+250 (^1H, 250.13 MHz; ^{13}C, 62.90 MHz, ^{11}B, 80.25 MHz), AVII+400 (^1H, 400.13 MHz; ^{13}C, 100.61 MHz, ^{19}F, 376.48 MHz), and Bruker AVII+500 spectrometers (^1H, 500.13 MHz; ^{13}C, 125.76 MHz). ^1H and ^{13}C shifts are referenced to internal solvent resonances and reported in parts per million relative to TMS. Coupling constants are given in Hertz. DRIFT IR spectra were recorded on a NICOLET 6700 FTIR spectrometer using dried KBr and KBr windows. For the latter the collected data were converted using the Kubelka−Munk refinement. Elemental analyses were performed on an Elementar Vario Micro Cube instrument. The molar masses (M_w and M_n) of the polymers were determined by size-exclusion chromatography (SEC). Sample solutions (1.0 mg of

DOI: 10.1021/acs.organomet.5b00589
Organometallics 2015, 34, 4994−5008

polymer/mL of THF) were filtered through a 0.45 mm syringe filter prior to injection. SEC was performed with a GPCmax VE2001 pump (Viscotek) by employing ViscoGEL columns. Signals were detected by using a triple detection array (TDA 305) and calibrated against polystyrene standards (M_w/M_n < 1.15). The flow rate was set to 1.0 mL min^{-1}. The microstructure of the polyisoprenes was examined by ^{1}H NMR and ^{13}C NMR spectroscopy in $CDCl_3$ at ambient temperature. $CDCl_3$ was purchased from Euriso-top and used as received.

General Procedure for $Ln_2(AlMe_4)_2(Ndipp)_2(AlMe_3)$. A solution of $Ln(AlMe_4)_3$ (**1**) in 3 mL of toluene was added to a vigorously stirred suspension of lithium (2,6-diisopropylphenyl)amide (**2**; Li(HNdipp)) in 2 mL of toluene. Instant gas formation was observed. The reaction mixture was stirred for 2 h at ambient temperature, 2 mL of *n*-hexane was added, and the solution was then separated by centrifugation, decanted, and filtered. The solid residue (product and $Li[Al(CH_3)_4]$) was extracted with additional toluene/*n*-hexane (1/1, 3 × 3 mL). The filtrate was dried under vacuum and triturated with *n*-hexane (2 × 2 mL). Then, the solid was washed with *n*-hexane (5 × 1 mL), followed by drying under reduced pressure. Compounds **3**-Ln were obtained as powders or by crystallization at ambient temperature.

*$La_2(AlMe_4)_2(Ndipp)_2(AlMe_3)$ (**3**-La).* Following the procedure described above, $La(AlMe_4)_3$ (**1**; 240 mg, 0.60 mmol) and Li(HNdipp) (**2**; 110 mg, 0.60 mmol) gave **3**-La as a yellow powder (256 mg, 0.29 mmol, 98%, 22% crystallized yield). Colorless crystals suitable for X-ray structure analysis were obtained from yellow *n*-hexane or toluene/*n*-hexane solutions at ambient temperature. ^{1}H NMR (500 MHz, C_6D_6, 26 °C, TMS): δ 7.14 (d, $^3J_{HH}$ = 7.7 Hz, 2H, Ar, H_{meta}), 6.99 (d, $^3J_{HH}$ = 7.8 Hz, 2H, Ar, H_{meta}), 6.94 (t, $^3J_{HH}$ = 7.7 Hz, 1H, Ar, H_{para}), 6.84 (t, $^3J_{HH}$ = 7.7 Hz, 1H, Ar, H_{para}), 2.90 (s br, 2H, $CH(CH_3)_2$), 2.70 (sept, $^3J_{HH}$ = 6.5 Hz, 2H, $CH(CH_3)_2$), 1.12 (m, 24H, $CH(CH_3)_2$), 0.06 (s, 9H, $Al(CH_3)_3$), −0.46 (s, 24H, $Al(CH_3)_4$) ppm. ^{13}C NMR (126 MHz, C_6D_6, 26 °C): δ 149.1 (Ar, C_{ipso}), 144.4 (Ar, C_{ipso}), 143.7 (Ar, C_{ortho}), 129.1 (Ar, C_{meta}), 127.2 (Ar, C_{meta}), 124.0 (Ar, C_{para}), 123.5 (Ar, C_{para}), 33.4 ($CH(CH_3)_2$), 29.9 ($CH(CH_3)_2$), 24.7 ($CH(CH_3)_2$), 24.0 ($CH(CH_3)_2$), 3.56 ($Al(CH_3)_3$), 1.43 ($Al(CH_3)_4$) ppm. DRIFT (KBr): 3051 w, 2995 w, 2969 m, 2956 m, 2945 m, 2921 m, 2886 m, 2836 m, 2799 w, 1583 w, 1459 w, 1403 s, 1386 w, 1361 w, 1321 w, 1306 w, 1284 w, 1257 w, 1225 s, 1194 s, 1184 s, 1143 m, 1117 w, 1087 w, 1044 w, 924 w, 881 m, 859 m, 848 m, 796 w, 763 m, 695 vs, 622 w, 609 m, 569 m, 561 m, 546 m, 535 m, 517 m, 477 m, 435 w cm^{-1}. Anal. Calcd for $C_{35}H_{67}Al_3La_2N_2$ (874.68 g mol^{-1}): C, 48.06; H, 7.72; N, 3.20. Found: C, 48.29; H, 7.62; N, 3.26.

*$Ce_2(AlMe_4)_2(Ndipp)_2(AlMe_3)$ (**3**-Ce).* Following the procedure described above, $Ce(AlMe_4)_3$ (**1**; 80 mg, 0.20 mmol) and Li(HNdipp) (**2**; 37 mg, 0.20 mmol) gave **3**-Ce as an orange powder (75 mg, 0.09 mmol, 86%). Crystallization from an *n*-hexane solution at ambient temperature afforded yellow crystals suitable for X-ray diffraction analysis. ^{1}H NMR (500 MHz, C_6D_6, 26 °C, TMS): δ 23.37, 0.00, −5.05, −8.50, −15.26, −25.63 ppm. DRIFT (KBr): 2958 m, 2924 m, 2881 m, 1463 w, 1407 m, 1360 w, 1315 w, 1259 w, 1228 m, 1198 m, 1183 m, 1142 w, 1118 w, 883 w, 864 w, 847 w, 793 w, 759 m, 700 vs, 561 w, 531 w, 496 w, 477 w, 446 w, 403 w cm^{-1}. Anal. Calcd for $C_{35}H_{67}Al_3Ce_2N_2$ (877.10 g mol^{-1}): C, 47.93; H, 7.70; N, 3.19. Found: C, 47.84; H, 7.29; N, 3.23.

*$Nd_2(AlMe_4)_2(Ndipp)_2(AlMe_3)$ (**3**-Nd).* Following the procedure described above, $Nd(AlMe_4)_3$ (**1**; 299 mg, 0.74 mmol) and Li(HNdipp) (**2**; 135 mg, 0.74 mmol) yielded **3**-Nd as a green powder (299 mg, 0.34 mmol, 91%). ^{1}H NMR (400 MHz, C_6D_6, 26 °C, TMS): δ 29.0, 10.4, 10.0, 4.3, 3.3, −0.3, −7.6, −10.0, −10.3, −11.8, −14.0, −18.5, −54.2 ppm. DRIFT (KBr): 3056 vw, 2997 w, 2959 m, 2923 m, 2881 m, 2833 w, 1586 vw, 1464 w, 1407 m, 1386 w, 1360 w, 1316 w, 1302 vw, 1281 w, 1259 w, 1225 m, 1199 m, 1183 m, 1172 w, 1142 w, 1117 w, 1104 w, 1092 vw, 1043 vw, 1035 vw, 926 w, 884 w, 865 w, 847 w, 801 vw, 793 w, 758 m, 699 vs, 638 w, 625 w, 611 w, 571 w, 561 w, 551 w, 540 w, 529 w, 512 w, 497 w, 480 w, 448 w, 404 w cm^{-1}. Anal. Calcd for $C_{35}H_{67}Al_3N_2Nd_2$ (885.32 g mol^{-1}): C, 47.48; H, 7.63; N, 3.16. Found: C, 46.99; H, 7.42; N, 3.01.

*$[Y_2(AlMe_4)_2(Ndipp)_2(AlMe_3)]_n$ (**3**-Y).* Following the procedure described above, $Y(AlMe_4)_3$ (**1**; 35 mg, 0.10 mmol) and Li(HNdipp) (**2**; 18 mg, 0.10 mmol) yielded **3**-Y as a white powder (30 mg, 0.04 mmol, 77%). ^{1}H NMR (500 MHz, C_6D_6, 26 °C, TMS): δ 7.09 (d, $^3J_{HH}$ = 7.7 Hz, 2H, Ar, H_{meta}), 7.01 (d, $^3J_{HH}$ = 7.7 Hz, 2H, Ar, H_{meta}), 6.95 (t, $^3J_{HH}$ = 7.7 Hz, 1H, Ar, H_{para}), 6.84 (t, $^3J_{HH}$ = 7.8 Hz, 1H, Ar, H_{para}), 3.19 (sept, $^3J_{HH}$ = 6.7 Hz, 2H, $CH(CH_3)_2$), 2.46 (sept, $^3J_{HH}$ = 6.5 Hz, 2H, $CH(CH_3)_2$), 1.15 (d, $^3J_{HH}$ = 6.9 Hz, 24H, $CH(CH_3)_2$), 0.00 (t, $^2J_{YH}$ = 1.4 Hz, 9H, $Al(CH_3)_3$), −0.46 (d, $^2J_{YH}$ = 2.1 Hz, 24 H, $Al(CH_3)_4$) ppm. ^{13}C NMR (126 MHz, C_6D_6, 26 °C): δ 147.9 (Ar, C_{ipso}), 144.3 (t, $^2J_{YC}$ = 3.0 Hz, Ar, C_{ipso}), 142.0 (Ar, C_{ortho}), 129.1 (Ar, C_{meta}), 125.9 (Ar, C_{meta}), 123.6 (Ar, C_{para}), 123.4 (Ar, C_{para}), 34.3 ($CH(CH_3)_2$), 29.4 ($CH(CH_3)_2$), 26.1 ($CH(CH_3)_2$), 24.7 ($CH(CH_3)_2$), 1.77 ($Al(CH_3)_3$), −0.5 ($Al(CH_3)_4$) ppm. ^{1}H−^{89}Y HSQC NMR (25 MHz, C_6D_6, 26 °C): δ 405.64 ppm. DRIFT (KBr): 3056 vw, 2959 m, 2925 m, 2884 m, 1587 vw, 1457 w, 1408 m, 1385 w, 1362 w, 1316 w, 1258 w, 1231 m, 1184 m, 1143 w, 1114 w, 1039 vw, 925 vw, 884 w, 869 w, 848 w, 794 w, 773 w, 758 m, 701 vs, 566 m, 526 w, 491 w, 453 w, 413 w cm^{-1}. Anal. Calcd for $C_{35}H_{67}Al_3N_2Y_2$ (774.68 g mol^{-1}): C, 54.26; H, 8.72; N, 3.62. Found: C, 54.48; H, 8.53; N, 3.77.

Reaction of $La_2(AlMe_4)_2(Ndipp)_2(AlMe_3)$ (3-La) with $AlMe_3$: NMR Scale. $AlMe_3$ (8.7 mg, 0.12 mmol) was added to a J. Young NMR tube charged with **3**-La (17.5 mg, 0.02 mmol). The resulting yellow solution showed resonances indicative of $La(AlMe_4)_3$ (^{1}H NMR (400 MHz, C_6D_6, 26 °C, TMS): δ −0.19 ppm) and $[MeAl{-}Ndipp]_3$ (^{1}H NMR (400 MHz, C_6D_6, 26 °C, TMS): δ 7.0 (m, 3H, Ar), 3.56 (spt, $^3J_{HH}$ = 6.7 Hz, 2H, $CH(CH_3)_2$), 1.20 (d, $^3J_{HH}$ = 6.7 Hz, 12H, $CH(CH_3)_2$), −0.60 (s br, 3H, Al−CH_3, overlapping with resonances of **1**-La and $AlMe_3$) ppm).

*$La_2[N(SiMe_3)_2]_2(Ndipp)_2(AlMe_3)$ (**4**-La).* To a vigorously stirred chilled solution (−35 °C) of **3**-La (88 mg, 0.10 mmol) in toluene (1 mL) was added a cold solution (−35 °C) of $K[N(SiMe_3)_2]$ (40 mg, 0.2 mmol). The reaction mixture was stirred for 1 h at −35 °C. The product was separated by centrifugation and additionally filtered, and the volume of the solubles was reduced in vacuo to approximately 1 mL. Colorless crystals of **4**-La suitable for X-ray diffraction were obtained at −35 °C (29 mg, 0.028 mmol, 28%). ^{1}H NMR (500 MHz, C_6D_6, 26 °C, TMS): δ 7.15 (d, overlapping with C_6D_6, 2H, Ar, H_{meta}), 7.12 (d, $^3J_{HH}$ = 7.6 Hz, 2H, Ar, H_{meta}), 6.91 (t, $^3J_{HH}$ = 7.7 Hz, 1H, Ar, H_{para}), 6.87 (t, $^3J_{HH}$ = 7.6 Hz, 1H, Ar, H_{para}), 3.34 (spt, $^3J_{HH}$ = 6.7 Hz, 2H, $CH(CH_3)_2$), 2.96 (spt, $^3J_{HH}$ = 6.6 Hz, 2H, $CH(CH_3)_2$), 1.36 (d, $^3J_{HH}$ = 6.7 Hz, 12H, $CH(CH_3)_2$), 1.23 (d, $^3J_{HH}$ = 6.8 Hz, 12H, $CH(CH_3)_2$), 0.07 (s, 45H, $Si(CH_3)_3$, $Al(CH_3)_3$) ppm. ^{13}C{^{1}H} NMR (126 MHz, C_6D_6, 26 °C): δ 151.8 (Ar, C_{ipso}), 146.7 (Ar, C_{ipso}), 139.9 (Ar, C_{ortho}), 139.5 (Ar, C_{ortho}), 128.0 (Ar, C_{meta}, overlapping with C_6D_6), 125.7 (Ar, C_{meta}), 120.9 (Ar, C_{para}), 120.6 (Ar, C_{para}), 32.1 ($CH(CH_3)_2$), 29.2 ($CH(CH_3)_2$), 25.5 ($CH(CH_3)_2$), 24.6 ($CH(CH_3)_2$), 4.8 ($Si(CH_3)_3$), 3.9 ($Al(CH_3)_3$) ppm. DRIFT (KBr): 3049 vw, 2949 s, 2891 m, 1583 vw, 1558 vw, 1457 w, 1402 s, 1356 w, 1312 w, 1286 w, 1244 vs, 1224 s, 1196 m, 1182 m, 1139 w, 1112 w, 1093 vw, 999 vs, 925 w, 866 vs, 847 vs, 827 vs, 794 w, 757 vs, 694 s, 675 s, 595 m, 560 m, 478 w, 443 w cm^{-1}. Anal. Calcd for $C_{39}H_{79}AlLa_2N_4Si_4 \cdot 0.5C_7H_8$ (1021.21 g mol^{-1}): C, 47.83; H, 7.84; N, 5.25. Found: C, 47.52; H, 7.36; N, 5.29.

*$La_2(AlMe_4)(Cp')(Ndipp)_2(AlMe_3)$ (**5**-La).* To a vigorously stirred suspension of $KC_5Me_4SiMe_3$ (23 mg, 0.10 mmol) in toluene (1 mL) was added a solution of **3**-La (88 mg, 0.10 mmol) in toluene (3 mL). No color change was observed. The reaction mixture was stirred for 2 h at ambient temperature. After centrifugation the supernatants were filtered and dried under vacuum. The residue was washed with cold *n*-hexane (2 × 1 mL) and dried in vacuo. Single crystals suitable for X-ray diffraction were harvested from a saturated toluene solution at −35 °C (85 mg, 0.087 mmol, 87%; 51% crystallized yield). ^{1}H NMR (500 MHz, C_6D_6, 26 °C, TMS): δ 7.20 (d, $^3J_{HH}$ = 7.7 Hz, 2H, Ar, H_{meta}), 6.99 (d, $^3J_{HH}$ = 7.7 Hz, 2H, Ar, H_{meta}), 6.96 (t, $^3J_{HH}$ = 7.7 Hz, 1H, Ar, H_{para}), 6.84 (t, $^3J_{HH}$ = 7.7 Hz, 1H, Ar, H_{para}), 2.72 (m, 4H, $CH(CH_3)_2$), 2.19 (s br, 6H, $C_5Me_4SiMe_3$), 1.90 (s, 6H, $C_5Me_4SiMe_3$), 1.23 (d, $^3J_{HH}$ = 6.5 Hz, 6H, $CH(CH_3)_2$), 1.17 (d, $^3J_{HH}$ = 6.5 Hz, 6H, $CH(CH_3)_2$), 1.11 (d, $^3J_{HH}$ = 6.6 Hz, 12H, $CH(CH_3)_2$), 0.41 (s, $^2J_{SiH}$ = 3.2 Hz, 9H, $C_5Me_4SiMe_3$), 0.01 (s, 9H, $Al(CH_3)_3$), −0.73 (s, 12H, $Al(CH_3)_4$) ppm. ^{13}C{^{1}H} NMR (126 MHz, C_6D_6, 26 °C): δ 149.0 (Ar, C_{ipso}), 144.9 (Ar, C_{ipso}), 143.2 (Ar, C_{ortho}), 141.6 (Ar, C_{ortho}), 130.6

DOI: 10.1021/acs.organomet.5b00589
Organometallics 2015, 34, 4994−5008

($C_5Me_4SiMe_3$), 127.2 (Ar, C_{meta}), 126.5 ($C_5Me_4SiMe_3$), 122.9 (Ar, C_{para}), 122.2 (Ar, C_{para}), 119.0 ($C_5Me_4SiMe_3$), 32.3 ($CH(CH_3)_2$), 31.7 ($CH(CH_3)_2$), 29.9 ($CH(CH_3)_2$), 25.1 ($CH(CH_3)_2$), 25.0 ($CH(CH_3)_2$), 23.4 ($CH(CH_3)_2$), 22.5 ($CH(CH_3)_2$), 15.4 ($C_5Me_4SiMe_3$), 14.7 ($C_5Me_4SiMe_3$), 12.1 ($C_5Me_4SiMe_3$), 2.5 ($Al(CH_3)_3$), 2.4 ($C_5Me_4SiMe_3$), 1.9 ($Al(CH_3)_4$) ppm. $^{29}Si\{^1H\}$ DEPT-45 NMR (99 MHz, C_6D_6, 26 °C, TMS): δ −11.69 ppm. DRIFT (KBr): 3056 vw, 2958 s, 2918 s, 2884 s, 2831 w, 1584 w, 1558 w, 1456 m, 1446 w, 1436 w, 1418 w, 1403 vs, 1386 w, 1323 m, 1284 w, 1257 m, 1248 m, 1227 vs, 1197 s, 1159 w, 1142 w, 1121 w, 1095 w, 1035 vw, 1014 vw, 926 vw, 882 m, 849 vs, 794 w, 760 s, 702 vs, 688 vs, 638 w, 626 w, 607 w, 581 m, 564 m, 556 m, 517 w, 502 w, 474 w, 457 w, 444 w, 436 w, 404 m cm^{-1}. Anal. Calcd for $C_{43}H_{76}Al_2La_2N_2Si$ (980.94 g mol^{-1}): C, 52.65; H, 7.86; N, 2.86. Found: C, 52.79; H, 7.87; N, 2.85.

*$La_2(Cp')_2(Ndipp)_2(AlMe_3)$ (**6**-La).* To a stirred solution of **3**-La (70 mg, 0.08 mmol) in toluene (1 mL) was added a suspension of $KC_5Me_4SiMe_3$ (37 mg, 0.16 mmol) in toluene (2 mL). The yellow reaction mixture was stirred for 2 h at ambient temperature. The product was separated by centrifugation and the solid residue extracted with *n*-hexane (1 mL). The combined extracts were filtered and dried under vacuum. Single crystals suitable for X-ray diffraction were obtained by crystallization at −35 °C from a saturated solution in toluene (87 mg, 0.08 mmol, quantitative; 11 mg, 13% crystallized yield). ^1H NMR (500 MHz, C_6D_6, 26 °C, TMS): δ 7.20 (d, $^3J_{HH}$ = 7.7 Hz, 2H, Ar, H_{meta}), 6.99 (d, $^3J_{HH}$ = 7.8 Hz, 2H, Ar, H_{meta}), 6.96 (t, $^3J_{HH}$ = 7.7 Hz, 1H, Ar, H_{para}), 6.84 (t, $^3J_{HH}$ = 7.7 Hz, 1H, Ar, H_{para}), 2.72 (m, 4H, $CH(CH_3)_2$), 2.19 (s, 6H, $C_5Me_4SiMe_3$), 1.90 (s, 6H, $C_5Me_4SiMe_3$), 1.23 (d, $^3J_{HH}$ = 6.1 Hz, 6H, $CH(CH_3)_2$), 1.17 (d, $^3J_{HH}$ = 6.6 Hz, 6H, $CH(CH_3)_2$), 1.11 (d, $^3J_{HH}$ = 6.7 Hz, 6H, $CH(CH_3)_2$), 0.41 (s, $^1J_{CH}$ = 60.1 Hz, $^2J_{SiH}$ = 3.3 Hz, 9H, $C_5Me_4SiMe_3$), 0.01 ($Al(CH_3)_3$), −0.73 ($Al(CH_3)_4$) ppm. $^{13}C\{^1H\}$ NMR (126 MHz, C_6D_6, 26 °C): δ 153.3 (Ar, C_{ipso}), 149.8 (Ar, C_{ortho}), 130.7 ($C_5Me_4SiMe_3$), 126.3 (Ar, C_{meta} and $C_5Me_4SiMe_3$), 119.1 ($C_5Me_4SiMe_3$), 118.8 (Ar, C_{para}), 118.7 (Ar, C_{para}), 30.22 ($CH(CH_3)_2$), 25.1 ($CH(CH_3)_2$), 15.2 ($C_5Me_4SiMe_3$), 12.3 ($C_5Me_4SiMe_3$), 6.5 ($Al(CH_3)_3$), 3.0 ($C_5Me_4SiMe_3$) ppm. $^{29}Si\{^1H\}$ DEPT-45 NMR (99 MHz, C_6D_6, 26 °C, TMS): δ −11.38 ppm. DRIFT (KBr): 3038 vw, 2952 s, 2929 m, 2899 m, 2865 m, 1588 vw, 1579 vw, 1539 vw, 1456 w, 1394 s, 1360 w, 1323 m, 1312 m, 1250 s, 1224 vs, 1198 s, 1140 w, 1096 vw, 1040 w, 1016 vw, 926 vw, 883 w, 844 vs, 836 vs, 791 vw, 753 s, 686 s, 639 vw, 630 w, 620 vw, 592 vw, 554 vw, 519 vw, 474 vw, 407 vw cm^{-1}. Anal. Calcd for $C_{51}H_{85}AlLa_2N_2Si_2$ (1087.18 g mol^{-1}): C, 56.34; H, 7.88; N, 2.58. Found: C, 56.30; H, 7.80; N, 2.62.

*$La_2(AlMe_4)_2(Ndipp)[NC_6H_3iPr(CMe_2)(AlMe_2)]$ (**7**-La).* To a vigorously stirred solution of **3**-La (70 mg, 0.08 mmol) in toluene (2 mL) was added THF (12 mg, 0.17 mmol). The yellow solution was stirred for 2 h at ambient temperature. The compound was dried under vacuum and washed with *n*-hexane (3 × 1 mL), followed by drying under reduced pressure. The title compound was obtained as a white powder (52 mg, 0.6 mmol, 80%). Crystallization from toluene at −35 °C afforded colorless crystals suitable for X-ray diffraction analysis. ^1H NMR (500 MHz, C_6D_6, 26 °C, TMS): δ 7.22 (d, $^3J_{HH}$ = 7.1 Hz, 2H, Ar, H_{meta}), 7.09 (d, $^3J_{HH}$ = 7.7 Hz, 2H, Ar, H_{meta}), 6.88 (t, $^3J_{HH}$ = 7.7 Hz, 1H, Ar, H_{para}), 6.68 (t, $^3J_{HH}$ = 7.7 Hz, 1H, Ar, H_{para}), 3.58 (s br, 1H, $CH(CH_3)_2$), 3.27 (m, 12H, $(CH_2)_2(CH_2)_2O$; residual THF solvent), 3.04 (sept, $^3J_{HH}$ = 6.8 Hz, 2H, $CH(CH_3)_2$), 1.27 (d, $^3J_{HH}$ = 6.7 Hz, 6H, $CH(CH_3)_2$), 1.23 (d, $^3J_{HH}$ = 7.3 Hz, 12H, $CH(CH_3)_2$), 1.13 [m, 18H, $CH(CH_3)_2$ and $[(CH_2)_2(CH_2)_2O$; residual THF solvent)], −0.13 (s, 3H, $Al(CH_3)$), −0.25 (s, 24H, $Al(CH_3)_4$), −0.39 (s, 3H, $Al(CH_3)$) ppm. $^{13}C\{^1H\}$ NMR from $^1H-^{13}C$ HSQC and HMBC (126 MHz, C_6D_6, 26 °C): δ 149.8 (Ar, C_{ipso}), 149.2 (Ar, C_{ipso}), 140.2 (Ar, C_{ortho}), 136.2 (Ar, C_{ortho}), 127.9 (Ar, C_{meta}), 126.6 (Ar, C_{meta}), 125.2 (Ar, C_{para}), 118.3 (Ar, C_{para}), 69.5 ($O(CH_2)$ (CH_2); residual THF solvent), 30.1 ($CH(CH_3)_2$), 29.4 ($CH(CH_3)_2$, $O(CH_2)(CH_2)$; residual THF solvent), 24.8 ($CH(CH_3)_2$), 24.0 ($CH(CH_3)_2$), 0.87 ($Al(CH_3)_4$), −1.16 ($Al(CH_3)$), −8.32 ($Al(CH_3)$) ppm. DRIFT (KBr): 3044 vw, 2957 s, 2918 s, 1582 w, 1457 m, 1401 s, 1357 w, 1316 m, 1257 m, 1229 vs, 1197 s, 1137 w, 1111 w, 1018 w, 927 vw, 883 m, 857 s, 793 w, 756 s, 692 s, 622 m, 567 m, 445 w cm^{-1}. Anal. Calcd for $C_{31}H_{54}Al_3La_2N_2{\cdot}C_7H_8$ (813.53 g mol^{-1}): C, 50.39; H, 6.90; N, 3.09. Found: C, 50.43; H, 7.21; N, 3.33.

General Procedure for $[La(AlMe_4)(Ndipp)(DMAP)]_x$ (8-Ln). To a vigorously stirred solution of **3**-Ln in toluene/*n*-hexane (1/1, 2 mL) was added a solution of DMAP in toluene/*n*-hexane (6 mL). The mixture turned orange (La)/red (Ce), and precipitation of an off-white (La)/orange-brown (Ce) solid was observed. The suspension was stirred for 2 h at ambient temperature. The product was separated by centrifugation, washed five times with 2 mL of toluene/*n*-hexane (1/1), and dried under vacuum to yield **8**-Ln as a powdery solid.

*$[La(AlMe_4)(Ndipp)(DMAP)]_x$ (**8**-La).* Following the procedure described above, **3**-La (350 mg, 0.40 mmol) and DMAP (147 mg, 1.20 mmol) gave **8**-La as a off-white solid (272 mg, 0.26 mmol, 65%). Crystallization from a toluene/THF solution at −35 °C afforded yellow crystals of **8**-La·THF suitable for X-ray diffraction analysis. ^1H NMR (500 MHz, THF-d_8, 26 °C, TMS): δ 8.09 (dd, $^3J_{HH}$ = 7.2 Hz, $^4J_{HH}$ = 4.4 Hz, 4H, DMAP, H_{ortho}), 6.90 (d, $^3J_{HH}$ = 7.5 Hz, 4H, Ar, H_{meta}), 6.70 (dd, $^3J_{HH}$ = 7.1 Hz, $^4J_{HH}$ = 4.1 Hz, 4H, DMAP, H_{meta}), 6.35 (t, $^3J_{HH}$ = 7.5 Hz, 2H, Ar, H_{para}), 3.88 (s br, 4H, $CH(CH_3)_2$), 3.07 (s, 12H, $N(CH_3)_2$, DMAP), 1.11 (d, $^3J_{HH}$ = , 24H, $CH(CH_3)_2$), −0.76 (s, 3H, $Al(CH_3)$), −0.93 (s, 9H, $Al(CH_3)_3$), −1.16 (s, 12H, $Al(CH_3)_4$) ppm. ^{13}C NMR (126 MHz, THF-d_8, 26 °C) from $^1H^{13}C$−HSQC and HMBC: δ 156.4 (NCHCHC, DMAP), 151.4 (Ar, C_{ipso}), 148.0 (NCHCHC, DMAP), 138.6 (Ar, C_{ortho}), 123.8 (Ar, C_{meta}), 114.7 (Ar, C_{para}), 107.3 (NCHCHC, DMAP), 39.0 ($N(CH_3)_2$), 35.9 ($Al(CH_3)$), 28.4 ($CH(CH_3)_2$), 25.4 ($CH(CH_3)_2$, −3.4 ($Al(CH_3)_3$), −8.4 ($Al(CH_3)_4$) ppm. DRIFT (KBr): 3043 vw, 2963 m, 2918 m, 2884 m, 2865 w, 2804 vw, 1612 vs, 1583 w, 1540 m, 1534 m, 1457 w, 1445 w, 1400 s, 1356 w, 1318 m, 1261 m, 1229 vs, 1203 w, 1173 w, 1139 vw, 1112 w, 1091 vw, 1061 w, 1049 w, 997 s, 884 w, 860 m, 809 m, 791 vw, 752 m, 729 w, 693 s, 661 w, 627 w, 568 w, 557 m, 540 w, 444 w cm^{-1}. Anal. Calcd for $C_{46}H_{78}Al_2La_2N_6{\cdot}0.5\ C_7H_8$ (1046.40 g mol^{-1}): C, 52.65; H, 7.49; N, 8.01. Found: C, 52.82; H, 7.24; N, 7.87.

*$[Ce(AlMe_4)(Ndipp)(DMAP)]_x$ (**8**-Ce).* Following the procedure described above, **3**-Ce (84 mg, 0.10 mmol) and DMAP (35 mg, 0.29 mmol) gave **8**-Ce as a ocher solid (63 mg, 0.06 mmol, 60%). ^1H NMR (500 MHz, C_6D_6, 26 °C, TMS): δ 9.15, 6.03, 2.12, −0.27, −0.63, −0.91, −1.30, −1.45, −2.05, −2.25 ppm. DRIFT IR (KBr): 3044 w, 2964 m, 2920 m, 2883, 2865 m, 2804 w, 1612 vs, 1583 w, 1540 m, 1533 m, 1457 w, 1445 w, 1401 s, 1356 w, 1318 m, 1262 m, 1229 vs, 1204 w, 1173 w, 1140 w, 1112 w, 1091 vw, 1061 w, 1047 m, 997 s, 885 w, 861 m, 809 m, 791 vw, 752 m, 729 w, 693 s, 661 w, 626 w, 573 w, 557 m, 540 w, 445 w cm^{-1}. Anal. Calcd for $C_{46}H_{78}Al_2Ce_2N_6$ (1048.40 g mol^{-1}): C, 54.39; H, 7.56; N, 7.69. Found: C, 53.97; H, 7.20; N, 7.83.

General Procedure for $[La(L)(Ndipp)(DMAP)]_2$ (9-Ln−11-Ln, L = $N(SiMe_3)_2$). To a vigorously stirred suspension of **8**-Ln in toluene (1 mL) was added a solution of KL in toluene (2 mL). The reaction mixture was stirred for 2 h at ambient temperature. After centrifugation the supernatant was decanted and the product extracted with toluene (1 mL). The combined extracts were filtered and dried in vacuo. The solid product was washed with *n*-hexane (2 × 2 mL) and dried under reduced pressure. Single crystals suitable for X-ray diffraction were obtained at −35 °C from a saturated solution in toluene.

*$[La\{N(SiMe_3)_2\}(Ndipp)(DMAP)]_2$ (**9**-La).* Following the procedure described above, **8**-La (52 mg, 0.05 mmol) and $K[N(SiMe_3)_2]$ (20 mg, 0.10 mmol) gave **9**-La as a yellow solid (54 mg, 0.045 mmol, 90%). ^1H NMR (500 MHz, C_6D_6, 26 °C, TMS): δ 8.40 (s br, 2H, DMAP, H_{ortho}), 7.31 (d, $^3J_{HH}$ = 7.7 Hz, 2H, Ar, H_{meta}), 6.87 (t, $^3J_{HH}$ = 7.5 Hz, 1H, Ar, H_{para}), 5.97 (d, $^3J_{HH}$ = 3.8 Hz, 2H, DMAP, H_{meta}), 3.99 (spt, $^3J_{HH}$ = 6.9 Hz, 2H, $CH(CH_3)_2$), 1.93 (s, 6H, $N(CH_3)_2$), 1.47 (d, $^3J_{HH}$ = 6.3 Hz, 12H, $CH(CH_3)_2$), 0.47 (s, 3H, $Si(CH_3)$), 0.30 (s, $^1J_{CH}$ = 25.4 Hz, $^2J_{SiH}$ = 3.1 Hz, 15H, $Si(CH_3)$) ppm. $^{13}C\{^1H\}$ NMR (126 MHz, C_6D_6, 26 °C): δ 155.1 (DMAP, C_{ortho}), 152.0 (Ar, C_{ipso}), 149.3 (DMAP, C_{para}), 139.0 (Ar, C_{ortho}), 125.2 (Ar, C_{meta}), 116.2 (Ar, C_{para}), 106.8 (DMAP, C_{meta}), 38.4 ($N(CH_3)_2$), 29.1 ($C(CH_3)_2$), 26.0 ($C(CH_3)_2$), 5.91 ($Si(CH_3)$), 5.50 ($Si(CH_3)$) ppm. $^{29}Si\{^1H\}$ DEPT-45 NMR (99 MHz, C_6D_6, 26 °C, TMS): δ −15.11 ppm. DRIFT (KBr): 3033 vw, 2946 s, 2865 w, 1615 vs, 1578 w, 1540 s, 1456 w,

DOI: 10.1021/acs.organomet.5b00589
Organometallics 2015, 34, 4994−5008

1446 w, 1417 w, 1396 s, 1354 w, 1313 w, 1253 s, 1231 vs, 1199 w, 1137 w, 1111 w, 1095 w, 1062 w, 1018 s, 1000 vs, 949 w, 871 s, 834 s, 817 s, 766 w, 750 s, 688 w, 666 w, 610 vw, 593 w, 560 w, 533 w, 459 w, 419 vw cm^{-1}. Anal. Calcd for $C_{50}H_{90}La_2N_8Si_4$ (1193.46 g mol^{-1}): C, 50.32; H, 7.60; N, 9.39. Found: C, 50.52; H, 7.53; N, 9.05.

*[Ce{N(SiMe$_3$)$_2$}(Ndipp)(DMAP)]$_2$ (**9**-Ce).* Following the procedure described above, **8**-Ce (105 mg, 0.10 mmol) and K[N(SiMe$_3$)$_2$] (40 mg, 0.20 mmol) gave **9**-Ce as a red solid (97 mg, 0.08 mmol, 81%). ^{1}H NMR (500 MHz, C_6D_6, 26 °C, TMS): δ 10.48, 2.50, 0.47, 0.18, 0.10, −0.69, −1.72, −2.41, −4.41 ppm. DRIFT (KBr): 3034 w, 2948 s, 2864 m, 1614 vs, 1580 m, 1536 s, 1445 m, 1398 s, 1353 w, 1314 m, 1231 vs, 1231 vs, 1198 m, 1135 w, 1110 w, 1094 w, 1062 w, 1001 vs, 949 w, 870 s, 855 s, 835 s, 750 s, 691 w, 664 m, 609 w, 593 w, 560 m, 532 w, 456 w cm^{-1}. Anal. Calcd for $C_{50}H_{90}Ce_2N_8Si_4$ (1195.88 g mol^{-1}): C, 50.22; H, 7.59; N, 9.37. Found: C, 50.48; H, 7.36; N, 9.01.

*[La(Cp′)(Ndipp)(DMAP)]$_2$ (**10**-La).* Following the procedure described above, **8**-La (52 mg, 0.05 mmol) and $KC_5Me_4SiMe_3$ (23 mg, 0.10 mmol) gave **10**-La as an orange powder (57 mg, 0.09 mmol, 91%). ^{1}H NMR (500 MHz, C_6D_6, 26 °C, TMS): δ 8.37 (s br, 2H, DMAP, H_{ortho}), 7.26 (d, $^3J_{HH}$ = 7.6 Hz, 2H, Ar, H_{meta}), 6.90 (t, $^3J_{HH}$ = 7.5 Hz, 1H, Ar, H_{para}), 6.07 (d, $^3J_{HH}$ = 3.1 Hz, 2H, DMAP, H_{meta}), 3.22 (s br, 2H, $CH(CH_3)_2$), 2.08 (s, 6H, $N(CH_3)_2$), 2.05 (s, 6H, $C_5Me_4SiMe_3$), 1.98 (s, 6H, $C_5Me_4SiMe_3$), 1.33 (d, $^3J_{HH}$ = 6.8 Hz, 12H, $CH(CH_3)_2$), 0.32 (s, $^1J_{CH}$ = 59.1 Hz, $^2J_{SiH}$ = 3.2 Hz, 9H, $C_5Me_4SiMe_3$) ppm. ^{13}C{^{1}H} NMR (126 MHz, C_6D_6, 26 °C): δ 154.4 (DMAP, C_{ortho}), 149.9 (Ar, C_{ipso}), 149.2 (DMAP, C_{para}), 129.1 ($C_5Me_4SiMe_3$), 128.3 ($C_5Me_4SiMe_3$), 124.7 (Ar, C_{meta}), 122.9 ($C_5Me_4SiMe_3$), 115.6 (Ar, C_{para}), 115.2 ($C_5Me_4SiMe_3$), 106.3 (DMAP, C_{meta}), 37.9 ($N(CH_3)_2$), 29.1 ($C(CH_3)_2$), 24.9 ($C(CH_3)_2$), 13.7 ($C_5Me_4SiMe_3$), 11.0 ($C_5Me_4SiMe_3$), 3.0 ($Si(CH_3)_3$) ppm. ^{29}Si-{^{1}H} DEPT-45 NMR (99 MHz, C_6D_6, 26 °C, TMS): δ −11.94 ppm. DRIFT IR (KBr): 3025 vw, 2952 s, 2918 m, 2863 m, 1583 w, 1546 m, 1534 m, 1444 m, 1397 vs, 1357 w, 1315 m, 1294 w, 1244 m, 1233 s, 1214 vs, 1184 s, 1142 w, 1104 w, 1064 vw, 1043 vw, 1000 s, 948 vw, 879 w, 844 vs, 833 s, 807 m, 747 s, 691 w, 682 w, 630 vw, 559 w, 545 vw, 532 w, 462 w, 420 vw cm^{-1}. Anal. Calcd for $C_{62}H_{96}La_2N_6Si_2$ (1259.45 g mol^{-1}): C, 59.13; H, 7.68; N, 6.67. Found: C, 59.62; H, 7.61; N, 6.62.

*[La(OAr)(Ndipp)(DMAP)]$_2$ (**11**-La).* Following the procedure described above, **8**-La (52 mg, 0.10 mmol) and KOAr (Ar = 2,6-di-*tert*-butyl-4-methylphenyl; 26 mg, 0.10 mmol) gave **11**-La as a yellow solid (66 mg, 0.10 mmol, quantitative). ^{1}H NMR (500 MHz, C_6D_6, 26 °C, TMS): δ 8.16 (s br, 2H, DMAP, H_{ortho}), 7.30 (d, $^3J_{HH}$ = 7.5 Hz, 2H, Ar, H_{meta}), 7.19 (t, $^3J_{HH}$ = 7.5 Hz, 1H, dipp, H_{para}), 6.88 (s, 2H, Ar, H_{meta}), 5.87 (d, $^3J_{HH}$ = 5.2 Hz, 2H, DMAP, H_{meta}), 3.93 (spt, $^3J_{HH}$ = 6.8 Hz, 2H, *CH*, *i*Pr), 2.35 (s, 3H, {$(CH_3)_3C$}$_2C_6H_2(CH_3)$), 1.93 (s, 6H, $N(CH_3)_2$), 1.61 (s, 18H, {$(CH_3)_3C$}$_2C_6H_2(CH_3)$), 1.39 (d, $^3J_{HH}$ = 6.8 Hz, 12H, {$(CH_3)_2CH$}$_2C_6H_3$)ppm. ^{13}C{^{1}H} NMR (126 MHz, C_6D_6, 26 °C): δ 163.4 ({$(CH_3)_3C$}$_2C_6H_2(CH_3)$, C_{ipso}), 155.2 (DMAP, C_{ortho}), 152.1 ({$(CH_3)_2CH$}$_2C_6H_3$, C_{ipso}), 149.0 (DMAP, C_{para}), 138.4 ({$(CH_3)_2CH$}$_2C_6H_3$, C_{ortho}), 137.6 ({$(CH_3)_3C$}$_2C_6H_2(CH_3)$, C_{ortho}), 125.8 ({$(CH_3)_3C$}$_2C_6H_2(CH_3)$, C_{meta}), 125.1 ({$(CH_3)_2CH$}$_2C_6H_3$, C_{meta}), 122.4 ({$(CH_3)_3C$}$_2C_6H_2(CH_3)$, C_{para}), 116.0 ({$(CH_3)_2CH$}$_2C_6H_3$, C_{para}), 106.8 (DMAP, C_{meta}), 38.4 ($N(CH_3)_2$), 35.1 ($C(CH_3)_3$), 32.0 ($C(CH_3)_3$), 29.8 ($C(CH_3)_2$), 25.3 ($C(CH_3)_2$), 22.1 ({$(CH_3)_3C$}$_2C_6H_2(CH_3)$) ppm. DRIFT (KBr): 3037 vw, 2953 s, 2915 m, 2864 w, 1613 vs, 1580 w, 1537 w, 1457 w, 1444 w, 1419 s, 13965, 1353 vw, 1308 vw, 1258 s, 1232 vs, 1136 vw, 1112 vw, 1062 vw, 1000 s, 949 vw, 883 vw, 859 vw, 850 vw, 824 m, 805 m, 751 w, 731 vw, 693 vw, 564 vw, 533 vw, 512 w, 441 vw cm^{-1}. Anal. Calcd for $C_{68}H_{100}La_2N_6O_2{\cdot}C_6D_6$ (655.69 g mol^{-1}): C, 63.69; H, 8.09; N, 6.02. Found: C, 63.44; H, 8.53; N, 5.90.

*[Ce(OAr)(Ndipp)(DMAP)]$_2$ (**11**-Ce).* Following the procedure described above, **8**-Ce (53 mg, 0.10 mmol) and KOAr (26 mg, 0.10 mmol) gave **11**-Ce as a dark red solid (62 mg, 0.094 mmol, 94%). ^{1}H NMR (500 MHz, C_6D_6, 26 °C, TMS): δ 21.15, 11.37, 10.46, −0.13, −3.47, −5.42, −19.52 ppm. DRIFT IR (KBr): 2954 s, 2916 m, 2865 w, 1612 vs, 1580 vw, 1535m 1458 w, 1444 m, 1418 s, 1397 m, 1354 w, 1309 vw, 1258 s, 1233 vs, 1197 w, 1112 vw, 1000 s, 884 vw, 860 w, 850 w, 825 m, 805 m, 751 w, 565 w, 532 w, 514 w, 464 w, 444 w cm^{-1}. Anal. Calcd for $C_{68}H_{100}Ce_2N_6O_2$ (1313.79 g mol^{-1}): C, 62.17; H, 7.67; N, 6.40 found: C, 62.83; H, 7.19; N, 6.16.

General Procedure for the Preparation of Cationic Complexes. To a solution of **3**-La in C_6D_6 was added a solution or suspension of the cocatalyst ($[Ph_3C][B(C_6F_5)_4]$ or $[PhNMe_2H][B(C_6F_5)_4]$) in C_6D_6. The solution was transferred into a Teflon-valved type NMR tube.

*La$_2$(AlMe$_4$)$_2$(Ndipp)$_2$(AlMe$_3$) (**3**-La) with [Ph$_3$C][B(C$_6$F$_5$)$_4$].* Following the procedure described above, **3**-La (17.5 mg, 0.02 mmol) and $[Ph_3C][B(C_6F_5)_4]$ (18.4 mg, 0.02 mmol) gave a clear yellow solution after several minutes of mixing. ^{1}H NMR (400 MHz, C_6D_6): δ 7.13−6.82 (m, 21H, Ph_3CMe, Ar), 3.57, 2.86, 2.75, 2.57 (m, 4H, $(CH_3)_2CH$), 2.04 (s, 3H, Ph_3CMe), 1.21, 1.07 (m, 24H, $(CH_3)_2CH$), −0.02 (s, 9H, $Al(CH_3)_3$), −0.14, −0.19, −0.41 (s, 21H, free $Al(CH_3)_3$, $Al(CH_3)_4$). ^{11}B{^{1}H} NMR (80 MHz, C_6D_6): δ −16.0 ppm. ^{19}F{^{1}H} NMR (376 MHz, C_6D_6): δ −131.9 (s br, $\Delta_{1/2}$ = 45 Hz, F_{ortho}), −161.6 (t, $^3J_{FF}$ = 21 Hz, F_{para}), −165.8 (m, F_{meta}) ppm.

*La$_2$(AlMe$_4$)$_2$(Ndipp)$_2$(AlMe$_3$) (**3**-La) with [PhNMe$_2$H][B(C$_6$F$_5$)$_4$].* Following the procedure described above, **3**-La (17.5 mg, 0.02 mmol) and $[PhNMe_2H][B(C_6F_5)_4]$ (16.0 mg, 0.02 mmol) gave a faint colorless solution after several minutes of mixing. ^{1}H NMR (400 MHz, C_6D_6): δ 7.13 (d, $^3J_{HH}$ = 7.7 Hz, 4H, Ar, H_{meta}), 6.99−6.81 (m, 7H, Ph, Ar), 2.81 (s, 2H, $(CH_3)_2CH$), (spt, $^3J_{HH}$ = 6.4 Hz, $(CH_3)_2CH$), 2.26 (s, 6H, NMe_2), 1.11−1.07 (m, 24H, $(CH_3)_2CH$), 0.16 (s, CH_4), 0.01 (s, 9H, $Al(CH_3)_3$), −0.47 (s, 12H, $Al(CH_3)_4$), −0.54 (s, 9H, released $Al(CH_3)_3$) ppm. ^{11}B{^{1}H} NMR (80 MHz, C_6D_6): δ −16.5 ppm. ^{19}F{^{1}H} NMR (376 MHz, C_6D_6): δ −131.9 (m, F_{ortho}), −161.6 (t, $^3J_{FF}$ = 21 Hz, F_{para}), −165.8 (m, F_{meta}) ppm.

Detailed Polymerization Procedure. Run 5 in Table 2 is described as a typical example. To a solution of **3**-Ce (17.5 mg, 0.02 mmol) in toluene (8 mL) was added 1 equiv of $[Ph_3C][B(C_6F_5)_4]$ (18.4 mg, 0.02 mmol), and the mixture stood at ambient temperature for 5 min. After the addition of the catalyst mixture to isoprene (1.362 g, 20 mmol) the polymerization was carried out at ambient temperature for 24 h. The polymerization mixture was poured onto a large quantity of methanol containing 0.1% (w/w) 2,6-di-*tert*-butyl-4-methylphenol as a stabilizer. The polymer was washed with methanol and dried under vacuum at ambient temperature to constant weight. The polymer yield was determined gravimetrically.

■ ASSOCIATED CONTENT

Ⓢ Supporting Information

The Supporting Information is available free of charge on the ACS Publications website at DOI: 10.1021/acs.organomet.5b00589. CCDC 1410220−1410232 also contain supplementary crystallographic data for this paper.

Additional experimental procedures and spectroscopic and crystallographic data (PDF)
Crystallographic data (CIF)

■ AUTHOR INFORMATION

Corresponding Author

*E-mail for R.A.: reiner.anwander@uni-tuebingen.de.

Author Contributions

All authors have given approval to the final version of the manuscript.

Notes

The authors declare no competing financial interest.

■ ACKNOWLEDGMENTS

We are grateful to the German Science Foundation for support (Grant: AN 238/15-1).

■ REFERENCES

(1) Summerscales, O. T.; Cloke, F. G. N.; Hitchcock, P. B.; Green, J. C.; Hazari, N. *Science* **2006**, *311*, 829−831.

(2) Balazs, G.; Cloke, F. G. N.; Green, J. C.; Harker, R. M.; Harrison, A.; Hitchcock, P. B.; Jardine, C. N.; Walton, R. *Organometallics* **2007**, *26*, 3111−3119.
(3) Summerscales, O. T.; Jones, S. C.; Cloke, F. G. N.; Hitchcock, P. B. *Organometallics* **2009**, *28*, 5896−5908.
(4) Edelmann, A.; Lorenz, V.; Hrib, C. G.; Hilfert, L.; Blaurock, S.; Edelmann, F. T. *Organometallics* **2013**, *32*, 1435−1444.
(5) Duncan, A. P.; Bergman, R. G. *Chem. Rec.* **2002**, *2*, 431−445.
(6) Fout, A. R.; Kilgore, U. J.; Mindiola, D. J. *Chem. - Eur. J.* **2007**, *13*, 9428−9440.
(7) Chu, J.; Lu, E.; Liu, Z.; Chen, Y.; Leng, X.; Song, H. *Angew. Chem., Int. Ed.* **2011**, *50*, 7677−5680.
(8) Schrock, R. R.; Murdzek, J. S.; Bazan, G. C.; Robbins, J.; DiMare, M.; O'Regan, M. *J. Am. Chem. Soc.* **1990**, *112*, 3875−3886.
(9) Bazan, G. C.; Oskam, J. H.; Cho, H. N.; Park, L. Y.; Schrock, R. R. *J. Am. Chem. Soc.* **1991**, *113*, 6899−6907.
(10) Schrock, R. R.; Hoveyda, A. H. *Angew. Chem., Int. Ed.* **2003**, *42*, 4592−4633.
(11) Bolton, P. D.; Mountford, P. *Adv. Synth. Catal.* **2005**, *347*, 355−366.
(12) Zhang, S.; Nomura, K. *Catal. Surv. Asia* **2011**, *15*, 127−133.
(13) Giesbrecht, G. R.; Gordon, J. C. *Dalton Trans.* **2004**, 2387−2393.
(14) Summerscales, O. T.; Gordon, J. C. *RSC Adv.* **2013**, *3*, 6682−6692.
(15) Gade, L. H.; Mountford, P. *Coord. Chem. Rev.* **2001**, *216−217*, 65−97.
(16) Scott, J.; Basuli, F.; Fout, A. R.; Huffmann, J. C.; Mindiola, D. J. *Angew. Chem., Int. Ed.* **2008**, *47*, 8502−8505.
(17) Wicker, B. F.; Scott, J.; Fout, A. R.; Pink, M.; Mindiola, D. J. *Organometallics* **2011**, *30*, 2453−2456.
(18) Wicker, B. F.; Fan, H.; Hickey, A. K.; Crestani, M. G.; Scott, J.; Pink, M.; Mindiola, D. J. *J. Am. Chem. Soc.* **2012**, *134*, 20081−20096.
(19) Lu, E.; Chu, J.; Chen, Y.; Borzov, M. V.; Li, G. *Chem. Commun.* **2011**, *47*, 743−745.
(20) Chu, J.; Han, X.; Kefalidis, C. E.; Zhou, J.; Maron, L.; Leng, X.; Chen, Y. *J. Am. Chem. Soc.* **2014**, *136*, 10894−10897.
(21) Gerber, L. C. H.; Le Roux, E.; Törnroos, K. W.; Anwander, R. *Chem. - Eur. J.* **2008**, *14*, 9555−9564.
(22) Litlabø, R.; Zimmermann, M.; Saliu, K.; Takats, J.; Törnroos, K. W.; Anwander, R. *Angew. Chem., Int. Ed.* **2008**, *47*, 9560−9564.
(23) Scott, J.; Fan, H.; Wicker, B. F.; Fout, A. R.; Baik, M.-H.; Mindiola, D. J. *J. Am. Chem. Soc.* **2008**, *130*, 14438−14439.
(24) Zimmermann, M.; Takats, J.; Kiel, G.; Törnroos, K. W.; Anwander, R. *Chem. Commun.* **2008**, 612−614.
(25) Venugopal, A.; Kamps, I.; Bojer, D.; Berger, R. J. F.; Mix, A.; Willner, A.; Neumann, B.; Stammler, H.-G.; Mitzel, N. W. *Dalton Trans.* **2009**, 5755−5765.
(26) Bojer, D.; Neumann, B.; Stammler, H.-G.; Mitzel, N. W. *Chem. - Eur. J.* **2011**, *17*, 6239−6247.
(27) Bojer, D.; Venugopal, A.; Mix, A.; Neumann, B.; Stammler, H.-G.; Mitzel, N. W. *Chem. - Eur. J.* **2011**, *17*, 6248−6255.
(28) Huang, W.; Carver, C. T.; Diaconescu, P. L. *Inorg. Chem.* **2011**, *50*, 978−984.
(29) Kratsch, J.; Roesky, P. W. *Angew. Chem., Int. Ed.* **2014**, *53*, 376−383.
(30) Dietrich, H. M.; Grove, H.; Törnroos, K. W.; Anwander, R. *J. Am. Chem. Soc.* **2006**, *128*, 1458−1459.
(31) Bojer, D.; Venugopal, A.; Neumann, B.; Stammler, H. G.; Mitzel, N. *Angew. Chem., Int. Ed.* **2010**, *49*, 2611−6214.
(32) Evans, W. J.; Ansari, M. A.; Ziller, J. W.; Khan, S. I. *Inorg. Chem.* **1996**, *35*, 5435−5444.
(33) Gordon, J. C.; Giesbrecht, G. R.; Clark, D. L.; Hay, P. J.; Keogh, D. W.; Poli, R.; Scott, B. L.; Watkin, J. G. *Organometallics* **2002**, *21*, 4726−4734.
(34) Schädle, C.; Schädle, D.; Eichele, K.; Anwander, R. *Angew. Chem., Int. Ed.* **2013**, *52*, 13238−13242.
(35) Schädle, D.; Maichle-Mössmer, C.; Schädle, C.; Anwander, R. *Chem. - Eur. J.* **2015**, *21*, 662−670.
(36) Schädle, D.; Meermann-Zimmermann, M.; Schädle, C.; Maichle-Mössmer, C.; Anwander, R. *Eur. J. Inorg. Chem.* **2015**, *2015*, 1334−1339.
(37) Schädle, D.; Schädle, C.; Törnroos, K. W.; Anwander, R. *Organometallics* **2012**, *31*, 5101−5107.
(38) Evans, W. J.; Anwander, R.; Ziller, J. W. *Organometallics* **1995**, *14*, 1107−1109.
(39) Zimmermann, M.; Frøystein, N. Å.; Fischbach, A.; Sirsch, P.; Dietrich, H. M.; Törnroos, K. W.; Herdtweck, E.; Anwander, R. *Chem. - Eur. J.* **2007**, *13*, 8784−8800.
(40) Occhipinti, G.; Meermann, C.; Dietrich, H. M.; Litlabø, R.; Auras, F.; Törnroos, K. W.; Maichle-Mössmer, C.; Jensen, V. R.; Anwander, R. *J. Am. Chem. Soc.* **2011**, *133*, 6323−6337.
(41) Dietrich, H. M.; Schuster, O.; Törnroos, K. W.; Anwander, R. *Angew. Chem., Int. Ed.* **2006**, *45*, 4858−4863.
(42) Wells, R. L.; Rahbarnoohi, H.; Glaser, P. B.; Liable-Sands, L. M.; Rheingold, A. L. *Organometallics* **1996**, *15*, 3204−3209.
(43) Bezombes, J.-P.; Gehrhus, B.; Hitchcock, P. B.; Lappert, M. F.; Merle, P. G. *Dalton Trans.* **2003**, 1821−1829.
(44) Zimmermann, M.; Estler, F.; Herdtweck, E.; Törnroos, K. W.; Anwander, R. *Organometallics* **2007**, *26*, 6029−6041.
(45) Döring, C.; Kempe, R. *Eur. J. Inorg. Chem.* **2009**, *2009*, 412−418.
(46) Litlabø, R.; Lee, H. S.; Niemeyer, M.; Törnroos, K. W.; Anwander, R. *Dalton Trans.* **2010**, *39*, 6815−6825.
(47) Waggoner, K. M.; Hope, H.; Power, P. P. *Angew. Chem., Int. Ed. Engl.* **1988**, *27*, 1699−1700.
(48) Waggoner, K. M.; Power, P. P. *J. Am. Chem. Soc.* **1991**, *113*, 3385−3393.
(49) Choi, H.; Hwang, S. *Chem. Mater.* **1998**, *10*, 2323−2325.
(50) Cui, P.; Chen, Y.; Xu, X.; Sun, J. *Chem. Commun.* **2008**, 5547−5549.
(51) Cui, P.; Chen, Y.; Borzov, M. V. *Dalton Trans.* **2010**, *39*, 6886−6890.
(52) Lv, Y.; Xu, X.; Chen, Y.; Leng, X.; Borzov, M. V. *Angew. Chem., Int. Ed.* **2011**, *50*, 11227−11229.
(53) Evans, W. J.; Davis, B. L.; Ziller, J. W. *Inorg. Chem.* **2001**, *40*, 6341−6348.
(54) Holton, J.; Lappert, M. F.; Ballard, D. G. H.; Pearce, R.; Atwood, J. L.; Hunter, W. E. *J. Chem. Soc., Chem. Commun.* **1976**, 480−481.
(55) Dietrich, H. M.; Raudaschl-Sieber, G.; Anwander, R. *Angew. Chem., Int. Ed.* **2005**, *44*, 5303−5306.
(56) Jende, L. N.; Maichle-Mössmer, C.; Anwander, R. *Chem. - Eur. J.* **2013**, *19*, 16321−16333.
(57) Höfle, G.; Steglich, W.; Vorbrüggen, H. *Angew. Chem., Int. Ed. Engl.* **1978**, *17*, 569−583.
(58) Thomas, F.; Bauer, T.; Schulz, S.; Nieger, M. *Z. Anorg. Allg. Chem.* **2003**, *629*, 2018−2027.
(59) Tossell, J. A. *Organometallics* **2002**, *21*, 4523−4527.
(60) Zimmermann, M.; Törnroos, K. W.; Anwander, R. *Angew. Chem., Int. Ed.* **2007**, *46*, 3126−3130.
(61) Suh, S.; Guan, J.; Mîinea, L. A.; Lehn, J.-S. M.; Hoffman, D. M. *Chem. Mater.* **2004**, *16*, 1667−1673.
(62) Deacon, G. B.; Hamidi, S.; Junk, P. C.; Kelly, R. P.; Wang, J. *Eur. J. Inorg. Chem.* **2014**, *2014*, 460−468.
(63) Yang, Y.; Liu, B.; Lv, K.; Gao, W.; Cui, D.; Chen, X.; Jing, X. *Organometallics* **2007**, *26*, 4575−4584.
(64) Zhang, L.; Suzuki, T.; Luo, Y.; Nishiura, M.; Hou, Z. *Angew. Chem., Int. Ed.* **2007**, *46*, 1909−1913.
(65) Robert, D.; Spaniol, T. P.; Okuda, J. *Eur. J. Inorg. Chem.* **2008**, *2008*, 2801−2809.
(66) Zimmermann, M.; Törnroos, K.; Anwander, R. *Angew. Chem., Int. Ed.* **2008**, *47*, 775−778.
(67) Yang, Y.; Wang, Q.; Cui, D. *J. Polym. Sci., Part A: Polym. Chem.* **2008**, *46*, 5251−5262.
(68) Zhang, L.; Nishiura, M.; Yuki, M.; Luo, Y.; Hou, Z. *Angew. Chem., Int. Ed.* **2008**, *47*, 2642−2645.
(69) Robert, D.; Abinet, E.; Spaniol, T.; Okuda, J. *Chem. - Eur. J.* **2009**, *15*, 11937−11947.

DOI: 10.1021/acs.organomet.5b00589
Organometallics 2015, 34, 4994−5008

(70) Jende, L. N.; Hollfelder, C. O.; Maichle-Mössmer, C.; Anwander, R. *Organometallics* **2015**, *34*, 32−41.
(71) Kaita, S.; Hou, Z.; Wakatsuki, Y. *Macromolecules* **1999**, *32*, 9078−9079.
(72) Kaita, S.; Hou, Z.; Nishiura, M.; Doi, Y.; Kurazumi, J.; Horiuchi, A. C.; Wakatsuki, Y. *Macromol. Rapid Commun.* **2003**, *24*, 179−184.
(73) Kaita, S.; Doi, Y.; Kaneko, K.; Horiuchi, A. C.; Wakatsuki, Y. *Macromolecules* **2004**, *37*, 5860−5862.
(74) Zhang, L.; Luo, Y.; Hou, Z. *J. Am. Chem. Soc.* **2005**, *127*, 14562−14563.
(75) Li, H.; Marks, T. J. *Proc. Natl. Acad. Sci. U. S. A.* **2006**, *103*, 15295−15302.
(76) Motta, A.; Fragalà, I. L.; Marks, T. J. *J. Am. Chem. Soc.* **2009**, *131*, 3974−3984.
(77) Schröder, L.; Brintzinger, H.-H.; Babushkin, D. E.; Fischer, D.; Mülhaupt, R. *Organometallics* **2005**, *24*, 867−871.
(78) Chen, F.; Fan, S.; Wang, Y.; Chen, J.; Luo, Y. *Organometallics* **2012**, *31*, 3730−3735.
(79) Friebe, L.; Nuyken, O.; Obrecht, W. *Adv. Polym. Sci.* **2006**, 1−154.
(80) Fischbach, A.; Anwander, R. *Adv. Polym. Sci.* **2006**, 155−281.
(81) Zhang, Z.; Cui, D.; Wang, B.; Liu, B.; Yang, Y. *Molecular Catalysis of Rare-Earth Elements*; Springer: Berlin, Heidelberg, 2010; Vol. *137*, pp 49−108.
(82) Fischbach, A.; Klimpel, M. G.; Widenmeyer, M.; Herdtweck, E.; Scherer, W.; Anwander, R. *Angew. Chem., Int. Ed.* **2004**, *43*, 2234−2239.
(83) Fischbach, A.; Meermann, C.; Eickerling, G.; Scherer, W.; Anwander, R. *Macromolecules* **2006**, *39*, 6811−6816.
(84) Evans, P. A.; Stanley, A. L. *Synth. Commun.* **1995**, *25*, 515−519.
(85) Tsoureas, N.; Summerscales, O. T.; Cloke, F. G. N.; Roe, S. M. *Organometallics* **2013**, *32*, 1353−1362.

DOI: 10.1021/acs.organomet.5b00589
Organometallics 2015, 34, 4994−5008